



HAL
open science

On-tissue chemical derivatization reagents for matrix-assisted laser desorption/ionization mass spectrometry imaging

Mira Merdas, Mélanie Lagarrigue, Quentin Vanbellinghen, Thierry Umbdenstock, Georges da Violante, Charles Pineau

► To cite this version:

Mira Merdas, Mélanie Lagarrigue, Quentin Vanbellinghen, Thierry Umbdenstock, Georges da Violante, et al.. On-tissue chemical derivatization reagents for matrix-assisted laser desorption/ionization mass spectrometry imaging. *Journal of Mass Spectrometry*, 2021, 56 (10), 10.1002/jms.4731 . hal-03268385

HAL Id: hal-03268385

<https://hal.science/hal-03268385v1>

Submitted on 30 Jun 2021

HAL is a multi-disciplinary open access archive for the deposit and dissemination of scientific research documents, whether they are published or not. The documents may come from teaching and research institutions in France or abroad, or from public or private research centers.

L'archive ouverte pluridisciplinaire **HAL**, est destinée au dépôt et à la diffusion de documents scientifiques de niveau recherche, publiés ou non, émanant des établissements d'enseignement et de recherche français ou étrangers, des laboratoires publics ou privés.

On-tissue chemical derivatization reagents for MALDI mass spectrometry imaging

Mira Merdas^{1,2,3}, Mélanie Lagarrigue^{1,2}, Quentin Vanbellingen³, Thierry Umbdenstock³, Georges Da Violante³, Charles Pineau^{1,2*}

¹ Univ Rennes, Inserm, EHESP, Irset (Institut de Recherche en Santé, Environnement et Travail) – UMR_S 1085, F-35042 Rennes cedex, France

² Protim, Univ Rennes, F-35042 Rennes, France

³ Technologie Servier, 25/27 rue Eugène Vignat – CS 11749 – 45007 Orléans Cedex 1 – France

* To whom correspondence should be addressed: charles.pineau@inserm.fr

Short title: On-tissue chemical derivatization for MALDI MSI

Key words: MALDI mass spectrometry imaging, On-tissue Chemical Derivatization, sample preparation, sensitivity enhancement, exogenous and endogenous molecules

Abstract

Matrix-assisted laser desorption/ionization mass spectrometry imaging (MALDI MSI) is a key tool for the analysis of biological tissues. It provides spatial and quantitative information about different type of analytes within tissue sections. Despite the increasing improvements of this technique, the low detection sensitivity of some compounds remains an important challenge to overcome. Poor sensitivity is related to weak ionization efficiency, low abundance of analytes and matrix ions or endogenous interferences. On-tissue chemical derivatization (OTCD) has proven to be an important solution to these issues and is increasingly employed in MALDI MSI studies. OTCD reagents, synthesized or commercially available, have been essentially used for the detection of small exogeneous or endogenous molecules within tissues. Optimally, an OTCD reaction is performed in mild conditions, in an acceptable range

This article has been accepted for publication and undergone full peer review but has not been through the copyediting, typesetting, pagination and proofreading process which may lead to differences between this version and the Version of Record. Please cite this article as doi: 10.1002/jms.4731

of time, preserves the integrity of the tissues and prevents the delocalization. In addition to their reactivity with a targeted chemical function, some OTCD reagents can also be used as a matrix, which simplifies the sample preparation procedure. In this review, we present an exhaustive overview of OTCD reagents and methods used in MALDI MSI studies.

Introduction

Since its introduction in 1997 by Caprioli *et al.*¹, MALDI MSI has been applied to a large number of molecular species within biological tissues such as peptides², lipids³, glycans⁴, proteins⁵, and drugs⁶. A wide range of research fields were investigated through MALDI MSI studies such as pharmaceutical sciences⁷, clinical biomarkers discovery⁸, food analysis⁹, plant biology¹⁰, forensic sciences¹¹ and others. Indeed, MALDI MSI is a powerful technique that allows the mapping of different types of analytes within tissues without any prior knowledge, while preserving the spatial information along with the mass analysis. Moreover, MALDI MSI is a label free technique that provides distinction between a molecule of interest and its eventual metabolites or degradation products that may have different targets or toxicity than the parent molecule. In addition to the distribution information, significant advances have been made to obtain reliable quantification by MALDI MSI.^{12,13}

Despite these valuable advantages, the lack of sensitivity encountered in some cases in MALDI MSI represents a challenge. This can be caused by different factors: (1) the relative low abundance of the analytes of interest, (2) the low ionization yield of the analytes, which depends on their physicochemical characteristics, (3) the ion suppression effects caused by the competition between the analytes of interest and the complex environment constituted by the other molecules present within the tissue, (4) potential isobaric interferences from endogenous molecules or matrix ions.

During the last decades, different technological and instrumentation progresses have been proposed for MALDI MSI. Certain acquisition modes, such as continuous accumulation of selected ions (CASI), multiple reaction monitoring (MRM), and selective reaction monitoring (SRM), enables an improvement of the sensitivity of analyte detection. Ion mobility spectrometry (IMS) adds a separation dimension to the analysis by allowing isomer and isobar differentiation. It can thus improve the signal-to-noise ratio of low abundant analytes suffering from interferences. IMS is being increasingly used in MALDI MSI analysis and has been implemented in commercially available mass spectrometers.¹⁴ More recently, the introduction

of laser-induced post-ionization (MALDI-2) source has led to a remarkable enhancement of the sensitivity of MALDI MSI. This innovative technique requires a second laser fired orthogonally into the MALDI plume generated by the primary laser. This allows the detection of different compounds that don't ionize during conventional MALDI experiments.¹⁵ When combined with the transmission mode, MALDI-2 can also provide higher lateral resolutions, close to 1 μm .^{15, 16}

Another important aspect of MALDI MSI is the sample preparation that is a multi-step process crucial to obtain good quality results. The different steps from tissue sectioning to matrix deposition should be optimized to prevent analyte delocalization and obtain sensitive, robust and reproducible data. Different steps can be introduced to the sample preparation process to provide sensitive detection of target molecules. Among them, on-tissue chemical derivatization (OTCD) is increasingly employed in MALDI MSI studies to improve the detection of small endogenous and exogenous molecules within tissues.

Chemical derivatization has been widely used for liquid chromatography coupled to electrospray ionization mass spectrometry (LC-ESI-MS) analysis as a strategy to improve the ionization yield of poorly ionizable molecules.¹⁷ This technique has started to be applied in the field of MALDI MSI to efficiently detect analytes of interest directly from tissue sections. Indeed, OTCD enhances the detection sensitivity by adding a positively or negatively charged or easily protonated or deprotonated moiety to the analyte. Moreover, the modification of the m/z ratio induced by such derivatization can help in distinguishing the analytes of interest from isobaric interfering species corresponding to endogenous compounds or ions produced by conventional organic matrices in the low mass range. It can also be used for the stabilization of a chemical moiety in order to improve its detection and reduce its in-source or post-source decay. However, the application of chemical derivatization on tissue sections remains a challenge and presents several constraints. Ideally, the derivatization reaction should occur in mild conditions, prevent the delocalization of the analytes, preserve the integrity of the tissue, present a high reaction yield on tissue and provide reproducible results. Therefore, different elements must be taken into consideration to achieve this goal. Thus, the derivatization reagent should not present a labile character in water due to ice crystals formation during the cryosection. The concentration of the derivatization reagent should be balanced to obtain a high reaction rate while avoiding a signal extinction effect. The solvent

composition plays also a crucial role to solubilize and target analytes within tissues while preserving them from delocalization. Moreover, the reaction and incubation times should stay within an acceptable time range to prevent delocalization or degradation. Finally, the solubility of the reagent in matrix solvent is essential to achieve homogeneous co-crystallization and provide analysis at a high lateral resolution. In some cases, the OTCD reagent has a strong absorbance at the wavelength of the MALDI UV laser and can also be used as a reactive matrix. This enables the deposition of a single compound that can both selectively react with analytes and assist the MALDI desorption and ionization processes. The use of reactive matrices is a very attractive solution to simplify the sample preparation and minimizes the delocalization or degradation effects by limiting the wetting and incubation steps.

Derivatization reactions can be employed to target different type of chemical functions found in compounds suffering from low ionization efficiency, low mass abundance and isobaric interferences. For example, amine groups present in neurotransmitters and amino acids or ketone groups present in steroids can be targeted by OTCD protocols to significantly improve the detection sensitivity. In this review, we present the different OTCD protocols that can be employed to strongly improve the ionization yield of analytes, to enhance the selectivity and obtain structural information, or to stabilize some chemical moieties of targeted molecules. We also highlight different important aspects of OTCD protocols such as the use of reactive matrix and the optimization of some parameters such as incubation in solvent atmosphere, reaction temperature or the use of catalysts. In the sections of this review, we describe the use of different derivatization reagents on molecules bearing a particular chemical function such as amine, ketone, hydroxyl, double bond, etc.

1. Targeted chemical function: Amine

a. TAHS

The derivatization reagent *p*-*N,N,N*-trimethylammonioanilyl *N*-hydroxysuccinimidyl carbamate iodide (TAHS) was first synthesized by Shimbo *et al.*¹⁸ and used for sensitive analysis of amino acids by LC-ESI-MS/MS. The amino group of amino acids reacts with TAHS to form a ureido compound with a cationic charge under mild conditions (Table 1a). Toue *et al.*¹⁹ adapted TAHS derivatization to tissue sections in order to obtain information on the simultaneous spatial distribution of various amino acids and to compare normal liver to the metastatic and parenchymal regions of liver tissues from xenografts models of human colon

cancer. Without derivatization, several amino acids were undetectable by MALDI MSI due to significant matrix interferences and low ionization efficiencies. After optimization of the OTCD protocol, these amino acids, present at the levels of few micromoles per liter, were detected as TAHS derivatives in tissue sections. MALDI images of MS/MS fragment ions corresponding to the amino-acid derivatives were also provided, making their detection and imaging more accurate. The results showed quantities of free amino acids higher in the metastatic regions than parenchymal regions of tumor-bearing livers. The authors thus suggested that metabolic remodeling of the host tissue may be caused by the development of metastases. Arts *et al.*²⁰ also performed OTCD using TAHS reagent to enable a sensitive detection of many free amino acids and their labeled analogues. They presented a novel method based on stable isotope-labeling to study dynamic molecular changes of amino acids within tissues. They applied their method on hepatocellular metabolism of phenylalanine that is hydroxylated into tyrosine and whose altered levels are associated with liver diseases. The same OTCD protocol was applied by Wappler *et al.*²¹ to detect glutamine by MALDI MSI in tumor sections from patients with cholangiocarcinoma characterized by chemoresistance and poor prognosis. They showed that glutamine is heterogeneously distributed in the tumor specimens with a strong depletion inside the tumor compared to the benign tissues.

b. Cinnamaldehydes

The aldehyde group is known to react with primary amines to form a Schiff's base under mild conditions (Table 1b). *Trans*-cinnamaldehyde was first adapted to OTCD by Manier *et al.*²² to explore the penetration of isoniazid (INH), used as a treatment for tuberculosis, into lung tissues of infected and dosed rabbits. OTCD was used to modify the *m/z* ratio of INH that suffers from important endogenous interferences. They used MALDI targets precoated with the derivatization reagent to obtain a rapid OTCD of INH. The derivatized INH was then efficiently localized by tandem MALDI MSI in lung tissues. The signal intensity obtained by MALDI MSI for the derivatized INH was consistent with INH concentrations determined by LC-MS/MS. The precoating of MALDI targets with the derivatization reagent simplifies the sample preparation protocol, allows a homogeneous deposition of the reagent, limits the analyte delocalization and provides a rapid OTCD of the analyte. Manier *et al.*²³ applied the 4-hydroxy-3-methoxycinnamaldehyde (CA) derivatization to improve the detection of endogenous amine metabolites such as neurotransmitters and amino acids within tissues. Indeed,

MALDI MSI is a powerful technique to study neurotransmitters, it provides *in situ* visualization of analytes and information about their abundance without requiring labeling or prior knowledge. The authors also used MALDI plates precoated with CA and *trans*-4-hydroxy-3-methoxycinnamic acid matrix to further minimize the delocalization effect of analytes. The spatial distribution of derivatized glutamic acid, γ -aminobutyric acid (GABA), dopamine, norepinephrine, and epinephrine was determined in pig adrenal glands and rat cerebellum. MS/MS transitions and high mass resolving power were used to further increase the specificity. They presented an analytical strategy to identify the metabolites and distinguish them from isobaric compounds by introducing LC-MS/MS analysis of tissue extracts. Enomoto *et al.*²⁴ also used CA to detect GABA in *Drosophila melanogaster* head and distinguish it from its isomers through specific fragmentation of the derivatization product. They showed that the 2,4-diphenyl-pyranilium (DPP) reagent (section 1.c) could also enable the detection of GABA. However, DPP did not allow the distinction of GABA from its isomers such as 2-aminobutyric acid.

MALDI MSI is mainly used to study the distribution of different types of molecule within animal tissues. However, recent advances in MALDI MSI in terms of instrumentation and sample preparation allow this technique to be increasingly applied to plants biology field²⁵. The combination of MALDI MSI with OTCD protocols was used to increase the ionization efficiency of molecules within plant tissues. O'Neil *et al.*²⁶ thus employed CA derivatization to investigate differential amino-acid distribution in maize roots (B73 and Mo17) and their reciprocal hybrid maize genotypes. They showed that amino acids were weakly abundant in the center of the roots of B73 whereas Mo17 presented highly abundant amino acids in the root cortex. Both hybrid roots showed amino-acid abundance similar to that of the maternal parent. This example demonstrates the applicability of OTCD protocols on plant tissues.

c. **DPP-TFB**

Pyrylium salts react with primary amines to produce N-alkyl- or N-aryl-pyridinium derivatives (Table 1c). The reaction is selective, rapid and occurs under mild conditions, ambient temperature and atmospheric pressure. Several studies have reported the use of 2,4-diphenyl-pyranilium tetrafluoroborate (DPP-TFB) for the detection of amine containing compounds especially amino acids and neurotransmitters in biological tissues. Dilillo *et al.*²⁷ used the DPP-TFB to detect amino metabolites such as glycine, alanine, GABA, proline, valine and

many others in a murine model of glioblastoma multiforme by MALDI MSI. They compared tumor and healthy regions of the brain and thus confirmed the differential regulation of metabolites involved in different metabolic pathways, consistent with an increased proliferation. Eto *et al.*²⁸ studied the distribution of glutamate and GABA after derivatization with DPP-TFB in Scrapper knockout and wild-type mice tissue sections. Their results showed a differential and region-specific effect of Scrapper, a gene that regulates synaptic transmission, on the abundance of glutamate and GABA. The same group²⁹ also used this derivatization reagent to study the relative abundance and the distribution of glycine in mouse brain in order to better understand the pathogeneses related to glycine concentration disorders. They showed that the highest intensity of derivatized glycine was detected in the brain stem in both adults and developing mice. On the other hand, Sugiyama *et al.*³⁰ generated a murine atlas of serotonin, dopamine and norepinephrine by MALDI MSI after OTCD using the DPP-TFB. Their results provided details about monoamine distribution and the regional differences in serotonin metabolism in the brain of mice subjected to behavioral experiments. In another study, Sugiyama *et al.*³¹ detect dopamine and 3-methoxytyramine that is a post-synaptic metabolite generated after dopamine degradation in mouse brain tissue sections. The aim of this study was to evaluate the physiological role and biochemical process underlying the alteration of dopamine and 3-methoxytyramine levels within the nucleus accumbens after an optogenetic sensory nerve stimulation. They demonstrated that rapid and region-specific fluctuations of monoamine levels occur in response to a sensitized, and pain stimuli and might be associated with the development of mechanical allodynia. Similarly, Cao *et al.*³² applied the DPP-TFB on crustacean brain sections to detect multiple neurotransmitters, such as dopamine, serotonin, GABA, and histamine in crustacean brain sections. The authors verified the identities of the detected molecules by analyzing standards via LC-MS/MS. This work led to a better understanding of metabolic signaling in the crustacean nervous system. Finally, Enomoto *et al.*²⁴ developed the first optimized method to study the distribution of GABA in the adult head of *Drosophila melanogaster* by MALDI MSI. They used DPP-TFB for OTCD and showed that GABA is distributed all over the head except for the retina.

Pyrylium salts have the advantage of being employed as reactive matrices. This simplifies the sample preparation and minimizes the delocalization or degradation effects. Shariatgorji *et al.*³³ thus performed a study in which they demonstrated the efficiency of three pyrylium salts as reactive matrices to enhance the detection of dopamine, amphetamine, and the envi-

ronmental neurotoxin β -N-methylamino-L-alanine in mouse and rat brain tissue sections. They found that DPP was the most efficient reagent to enhance the signal intensity obtained for dopamine relative to 2,4,6-trimethyl-pyrylium (TMP) and 1,4-phenylene-4,4'-bis (2,6-diphenyl-4-pyrylium) (PBDPP). DPP was also used to localize substituted amphetamine and quantify β -N-methylamino-L-alanine. The same group³⁴ used DPP-TFB as a reactive matrix and TMP-TFB to simultaneously identify and quantify several neurotransmitters and amino-acid chemical messengers, such as tyrosine, tryptamine, dopamine, 3-methoxytyramine, serotonin, GABA, and others. They showed that GABA is detected in all brain structures at different intensity levels whereas the dopamine is abundant in the striatal region of rat brain (Figure 1). They also applied their method on brain tissue sections of primate and rodents with and without dopamine depletion and L-3,4-dihydroxyphenylalanine treatment to evaluate changes in the absolute and relative levels of neurotransmitters in different subregions of the brain.

Derivatization using pyrylium salts adds carbon and hydrogen to the target compounds and the resulting isotopic patterns of the product are not distinctive from molecules present in the tissue. Therefore, Shariatorji *et al.*³⁵ introduced a bromopyrylium salt (Br-TPP) to add the unique and highly recognizable isotope pattern of the halogen bromine to derivatized compounds. They applied TPP and Br-TPP to rat brain sections to evaluate the feasibility of this protocol and observed the distribution of derivatized dopamine, GABA, and a selective reuptake inhibitor drug, fluvoxamine. The use of a brominated reagent allowed the clear recognition of the isotopic pattern, thus facilitating the identification of derivatized and non-derivatized compounds in tissues. The authors showed the efficiency of this protocol in both MALDI and desorption electrospray ionization (DESI) MSI. DESI is a soft ionization source that offers the advantage of analyzing surfaces with no or little sample preparation. The ionization of target is achieved by directing a high velocity charged solvent spray onto the surface to be analyzed.³⁶ The advantage of DESI MSI is that derivatization reactions can be easily transferred from solution to tissue sections. In MALDI MSI more challenging elements must be taken into account to obtain a robust derivatization.³⁷

Comparison of TAHS, CA and DPP-TFB reagents

Esteve *et al.*³⁸ performed a comparison between the three derivatization reagents TAHS, CA, and DPP-TFB to visualize amino metabolites, such as neurotransmitters and amino acids.

This methodology was used for the detection of the alterations of amino metabolites in mouse brain after the induction of cortical spreading depression (CSD). They found that the maximum MALDI signals and the best spatial distribution were obtained with DPP-TFB. However, TAHS and CA showed better results in certain specific cases, such as negatively charged ions. The authors concluded that these derivatization reagents were complementary and that their combination provided the best results. They therefore applied a strategy combining the three derivatization reagents on mouse brain sections to visualize the distribution and alteration of up to 23 amino metabolites in the CSD model. Certain amino metabolites, such as GABA, alanine, serine, proline, valine, cysteine, leucine/isoleucine, lysine, phenylalanine, tyrosine, and tryptophan were detected with increased intensities in the CSD hemisphere. Aspartate and glutamate showed decreased intensities in the CSD hemisphere.

d. FMP-n

Fluoromethylpyridinium (FMP)-based reactive matrices that react with primary and secondary amine functions in nucleophilic aromatic substitution were synthesized by Shariatgorji *et al.*³⁹ (Table 1d). They presented an OTCD approach for the comprehensive mapping of neurotransmitter networks by MALDI MSI in tissue sections from Parkinson's disease rat and primate models, as well as tissues from human Parkinsonian brain. Various compounds of FMP were synthesized and tested such as 4-(10-bromoanthracen-9-yl)-2-fluoro-1-methylpyridin-1-ium iodide (FMP-8), 4-(Anthracen-9-yl)-2-fluoro-1-ethylpyridin-1-ium iodide (FMP-9) and 4-(Anthracen-9-yl)-2-fluoro-1-methylpyridin-1-ium iodide (FMP-10). Among these reagents, FMP-10 could be used as a reactive matrix and enabled the detection of dopamine and serotonin in rat brain at previously undetectable concentrations. They used the reactivity of FMP-10 with amines to map dopamine and its metabolites in different brain areas. One result showed the localization of derivatized dopamine and its metabolite, 3-methoxytyramine, to the ventral caudate nucleus of a Parkinsonian striatal human brain section, with higher levels observed in the medial division. In addition, the authors developed strategies for the identification of unknown molecules using a combination of MS/MS imaging on rat brain sections and the unique isotopic pattern of a brominated analog of FMP-10. Another group, Zhang *et al.*⁴⁰ investigated the role of GPR37, an orphan G-protein coupled receptor linked to the juvenile form of Parkinson's disease, in motor deficits. They used FMP-10 as a reactive matrix to derivatize dopamine and GABA in brain sections of GPR37 knock out and wild type mice

thus revealing an increase in GABA levels in GPR37 knock out striata after dopamine depletion. All the data provided by MALDI MSI and other techniques indicated that properly functional GPR37 may counteract aging process and Parkinson's disease.

e. NBA + hv

Li *et al.*⁴¹ developed a nanosecond photochemical reaction (nsPCR)-based click chemistry for the derivatization of primary amine groups in peptides and proteins. They introduced the 2-nitrobenzaldehyde (NBA) that generates the reactive 2-nitrosobenzoic anion (NS⁻) following nanosecond laser irradiation at wavelength of 355 nm (Table 1e). NS⁻ reacts with free primary amine groups spatially accessible in proteins and peptides resulting in a mass shift of 133 Da. They applied this strategy on mouse brain sections and enhanced the identification and visualization of neuropeptides.

f. mTRAQΔ0

mTRAQ® (mass differential tags for relative and absolute quantification) derivatization agents react with primary amines (Table 1f). Ito *et al.*⁴² used a group of mTRAQ including isotope-labeled analogues (mTRAQΔ0 and mTRAQΔ4). The authors applied a reproducible "triple spray" method to quantify GABA in rat brain sections. First, the mTRAQΔ0 was sprayed to derivatize endogenous amines. Then, before applying the matrix solution, the internal standard consisting of an amine standard derivatized with mTRAQΔ4 was sprayed and used for the normalization of the signal. This method was employed to quantitatively evaluate GABA in the hypothalamus, where it is known to be present at high concentrations and showed little variation (CV = 1.62%) due to the normalization on the internal standard.

g. 4-SPITC, 3-SBASE, TMPP

Franck *et al.*⁴³ evaluated various derivatization agents that react with N-terminal peptides (Table 1g), in order to enhance the identification of peptides detected by MS/MS after on-tissue trypsin digestion. N-terminal modifications are easier due to the strong reactivity of amines. The orientation of fragmentation toward specific series of fragment ions by derivatization simplifies the identification of the peptides. The authors used sulfonation agents, such as 4-sulphophenyl isothiocyanate (4-SPITC) and sulfobenzoic acid succinimidyl ester (3-SBASE), adding a negative charge to the N-termini of tryptic peptides, as well as *N*-

succinimidylloxycarbonylmethyl tris(2,4,6-trimethoxyphenyl) phosphonium bromide (TMPP), adding a positively charged moiety to the N-termini of tryptic peptides. The 3-SBASE derivatization reagent appeared to be more efficient than 4-SPITC due to the loss of 4-SPITC as a major fragmentation pathway observed on MS/MS spectra. Peptides corresponding to a fragment of myelin basic protein and tubulin R protein were thus both detected with a shifted mass upon derivatization with 3-SBASE. However, a number of difficulties with this derivatization reagent were encountered for peptides containing a missed cleavage. Moreover, derivatization by 3-SBASE required the presence of a basic amino-acid at the N-terminal position of the peptide. Derivatization with TMPP was also tested and has the advantage of being independent of the presence of a basic amino acid at the N-terminus of peptides, allowing the use of enzymes other than trypsin.

2. Targeted chemical function: Hydroxyl group

a. FMP-n

FMP-based reagents react not only with primary and secondary amines but also with hydroxyl groups in nucleophilic aromatic substitution (Table 2). Beasley *et al.*⁴⁴ reported the detection and mapping of cannabinoids in single hair samples after derivatization with FMP *p*-toluenesulfonate (FMPTS) that reacts with phenolic hydroxyl group in a nucleophilic aromatic substitution. Cannabis consumption is generally identified in hair samples by the detection of Δ^9 -tetrahydrocannabinol (THC), the main psychoactive constituent of cannabis, and its metabolites by standard analytical techniques, such as GC-MS and LC-MS. MALDI MSI provides advantages over conventional techniques, such as improved chronological information, simpler sample preparation, and the ability to detect drugs and their metabolites in a single hair. However, in-source rearrangement of THC and its low ionization yield prompted researchers to use a derivatization reagent. Thus, it was shown that the use of FMPTS enables the detection of cannabinoids and their metabolites, which have low ionization yields and endogenous interferences for some. Shariatgorji *et al.*³⁹ also apply the FMP-8,-9 and-10 reagents already described in the amine group section to enhance the detection of several neurotransmitters, including their metabolites, of the dopaminergic and serotonergic systems containing phenolic hydroxyl groups. They applied their strategy on brain tissue sections from a Parkinson's disease rat and primate model, as well as tissues of human Parkinsonian brain.

3. Targeted chemical function: Diol group

a. Boronic acid

Kaya *et al.*⁴⁵ used a synthesized 4-(*N*-methyl)pyridinium boronic acid (4-(*N*-Me)Py⁺B(OH)₂) as a derivatization reagent that reacts with the diol moiety of catecholamines (Table 3). This derivatization reagent worked as a reactive matrix and has been applied in combination with LDI-TOF and TOF-SIMS mass spectrometry techniques. The optimized OTCD protocol was employed as a proof of concept for the imaging of catecholamines such as dopamine, epinephrine, and norepinephrine in porcine adrenal gland tissue sections. Forsman *et al.*⁴⁶ used a commercially available boronic acid, the 4-(dimethylamino)phenylboronic acid (DBA), to react with vicinal diols. They applied this strategy to explore the metabolite coverage in maize stems, roots and leaves. Their results showed that dozens of vicinal diol metabolites were derivatized efficiently.

4. Targeted chemical function: Carbonyl group

a. GirT

The Girard T (GirT) reagent reacts with ketones by a hydrazine-type condensation reaction and provides a permanent positive charge to derivatized molecules (Table 412a). Several studies employed OTCD using GirT to detect essentially steroids due to their relative low abundance and poor ionization efficiency in MALDI which make their mapping by MSI challenging. Cobice *et al.*⁴⁷ optimized the OTCD method with GirT reagent for the direct quantification of corticosterone and 11-dehydrocorticosterone intracrinology in rat adrenal glands and mouse brain sections. Their results showed that a good correlation was obtained between quantifications provided by MSI, LESA, and LC-MS/MS. In addition, the CORT/11DHC ratio in the brain of mice with a 11 β -HSD1 enzyme (11 β -Hydroxysteroid dehydrogenase) deficiency or inhibition was determined. They observed a correlation between the regional activity of 11 β -HSD1 and the steroid quantity in brain subregions. Therefore, the authors⁴⁸ applied the same OTCD protocol to detect stable-isotope tracers (cortisol and cortisone) after an infusion of deuterated cortisol in mice. They evaluated the pharmacokinetics and pharmacodynamics of an 11 β -HSD1 inhibitor that access the brain. Indeed, small molecules inhibitors of 11 β -HSD1 must enter brain subregions, such as hippocampus to be effective for the treatment of dementia. They combined pharmacokinetic and pharmacodynamic analyses using tracer infusion and MSI and showed that the turnover of 11 β -HSD1 activity occurs in

liver and brain whereas it is absent in mice with genetic disruption *Hsd11b1* and inhibited by a 11β -HSD1 inhibitor drug.

Given the essential role of androgens in reproductive functions, OTCD with GirT was also used to localize and quantify testosterone and 5α -dihydrotestosterone in testis. Cobice *et al.*⁴⁹ showed that testosterone is mostly localized within seminiferous tubules, whereas 5α -dihydrotestosterone is detected in the interstitium and Leydig cells of rat testis at a lateral resolution of 50 μm (Figure 2). Shimma *et al.*⁵⁰ performed the microscopic visualization of testosterone in mouse testis sections after using two derivatization reagents: GirT and pyridine sulfur trioxide. The best results in terms of ionization efficiency, molecular specificity, and tissue preservation were obtained with the GirT reagent. They applied GirT derivatization to testis and showed an accumulation of testosterone at the surface of Leydig cells of treated mice with hCG, an activator agonist of the luteinizing hormone receptor. The quantification of underivatized testosterone in untreated and hCG-treated mouse testis by LC-MS/MS was in a good agreement with results obtained by MALDI MSI. Barré *et al.*⁵¹ used OTCD to study the distribution of triamcinolone acetonide in avascular cartilage. Triamcinolone acetonide is a synthetic corticosteroid used to treat pain and inflammation associated with osteoarthritis and is not easily detected by mass spectrometry due to its low ionization efficiency. Thus, the GirT reagent was selected in this study to enhance the sensitivity of triamcinolone acetonide detection. This method allowed evaluation of the distribution of TAA in human cartilage and its quantification using a deuterated TAA analogue.

Sugiura *et al.*⁵² used OTCD with GirT reagent analyses to visualize aldosterone and 18-oxocortisol in primary aldosteronism adrenal tissue sections from patients. They also combined OTCD to MS3 which allowed the differentiation of aldosterone and cortisone that share identical m/z ratio. Indeed, while MS2 did not produce specific signals, MS³ produced independent signals for aldosterone and cortisone GirT- aldosterone and cortisone. In addition, this strategy revealed that aldosterone and 18-oxocortisol co-accumulated within aldosterone synthase-expressing lesions. This result help to develop the hypothesis of an aldosterone-producing pathology in adrenal glands.

The study of the distribution of some plant hormones can contribute to a better understanding of their biological role in seeds. However, some molecules such as abscisic acid and 12-oxo-phytodienoic acid have been difficult to visualize by MALDI MSI due to their low ionization

efficiency. Thus, Enomoto *et al.*⁵³ performed OTCD using GirT reagent on *Phaseolus vulgaris* L seeds to detect these two hormones. MALDI MSI showed abscisic acid-GirT to be localized in the embryo, whereas 12-oxo-phytodienoic acid-GirT was observed in the external structures. These results were in accordance with those obtained previously by the same group with DESI-MSI, thus reflecting the complementarity of both techniques.

b. GirP

As GirT, the Girard P (GirP) reagent reacts with ketones by a hydrazine-type condensation reaction (Table 4b). Yutuc *et al.*⁵⁴ developed an on-tissue enzyme assisted derivatization combined with micro-liquid extraction surface analysis (LESA), MALDI MSI and LC-MS to visualize and quantify multiple sterols involved in the cholesterol metabolism in mouse brain. Indeed, cholesterol and its precursors and metabolites are important for proper brain functions. A dysregulation in cholesterol metabolism implicates several neurological disorders. As evocated, GirP provides hydrazine derivatization reaction for sterols possessing carbonyl function. However, some sterols do not possess carbonyl function, therefore, the authors used on-tissue enzymatic oxidation with cholesterol oxidase to form the carbonyl group prior to the derivatization with GirP. This method allowed the localization of oxysterols and cholesterol metabolites and showed differential distribution of cholesterol metabolites in subregions of the mouse brain.

c. DMNTH, DNPH

Flinders *et al.*⁵⁵ employed OTCD using hydrazine-based reagents to detect the carbonyl-containing compound (Table 4c), fluticasone propionate, a glucocorticoid used to treat asthma. Two reactive matrices were used for this study: 2,4-dinitrophenylhydrazine (DNPH) and 4-dimethylamino-6-(4-methoxy-1-naphthyl)-1,3,5-triazine-2-hydrazine (DMNTH). The improvement in sensitivity and the limit of detection was evaluated on a range of concentrations of fluticasone propionate (10 – 2000 ng/ μ L) spotted on rat lung tissue sections. The best results were obtained with DMNTH. The derivatization protocol was then further improved by extending the time of the reaction (~ 48 h) and the use of CHCA as an assistant matrix.

5. Targeted chemical function: Thiol group

a. CHC-Mal

Fülöp *et al.*⁵⁶ were interested in the detection of sulfur-containing proteins and metabolites. They reported the use of (E)-2-cyano-N-(2-(2,5-dioxo-2,5-dihydro-1H-pyrrol-1-yl)ethyl)-3-(4-hydroxyphenyl)-acrylamide (CHC-Mal), which can be considered to be a derivative of the MALDI matrix α -Cyano-4-hydroxycinnamic acid (CHCA) and can be used then as reactive matrix. CHC-Mal reacts selectively with free thiol groups (Table 5). The authors showed that CHC-Mal successfully derivatize reduced proteins, such as α and β chains of reduced insulin, in porcine pancreatic tissues. CHC-Mal was also able to contribute to the detection of small thiol-containing metabolites such as glutathione, cysteine and cysteinylglycine in porcine liver tissues. CHC-Mal not only facilitates the detection of the species within tissues but also prevents their oxidation.

6. Targeted chemical function: Carboxylic acid Group

a. 2-picolylamine

2-picolylamine reacts with the carboxylic acid group to form an amide bond in the presence of carboxylic acid activators 2,2-dipyridyl disulfide (DPDS) and triphenylphosphine (TPP) (Table 6a). Wu *et al.*⁵⁷ evaluated the electrospray deposition of derivatization reagents onto biological tissues to enhance the detection of free fatty acids. They demonstrated that OTCD using 2-picolylamine deposited by electrospray led to a three-fold improvement in the limit of detection and minimized the delocalization of analytes relative to airbrush deposition. Nine fatty acids including unsaturated and saturated fatty acids were detected and localized at a lateral resolution of 20 μm in different cell layers of the rat hippocampus.

b. DMPI

Wang *et al.*⁵⁸ synthesized *N,N*-dimethylpiperazineiodide (DMPI) that reacts with the carboxylic acid of free fatty acids in the presence of 2-(7-azabenzotriazol-1-yl)-*N,N,N',N'*-tetramethyluronium hexafluorophosphate (HATU) under mild conditions (Table 6b). Indeed, it has been shown that lipid metabolism is involved in malignancy during tumorigenesis. They developed an OTCD method that improved the detection of free fatty acids in thyroid cancer tissues. They showed thus the simultaneous detection of phospholipids detected without derivatization and derivatized fatty acids. The authors also studied the correlation between the intensities of detected phospholipids and free fatty acid derivatives in thyroid cancer samples using Spearman correlation analysis. The results showed a positive correlation

between saturated free fatty acids C16:0 and C18:0 and phospholipids, whereas the unsaturated free fatty acids showed different correlations with phospholipids in different tissue samples.

c. TMPA

Sun *et al.*⁵⁹ synthesized a new derivatization reagent, *N,N,N*-trimethyl-2-(piperazin-1-yl)ethan-1-aminium iodide (TMPA) that form stable amide bond with carboxylic acid containing compounds (Table 6c). They developed OTCD protocol using TMPA to detect carboxyl-containing metabolites (CCM). CCM are fundamental components of tissues and play key roles in cell energy metabolism and cell-cell signaling. Profiling CCM and linking their spatial distributions with tissue structures would provide a better understanding of metabolic networks. The authors tested various catalysts, temperatures, and solvents to optimize the OTCD reaction. Their results suggest that stronger MALDI MS signals can be obtained with the onium salt-based coupling reagent HATU/HBOt as a catalyst than with DPDS/TPP or EDC/HBOt. No significant impact of the temperature was mentioned. However, they demonstrated that solvents affect the efficiency of this reaction. The incubation in acetonitrile gas-phase solvent was shown to significantly increase the efficiency of OTCD of various derivatized CCM tested, without causing metabolite delocalization. They were able to detect a total of 28 CCM using the optimized protocol, including five tricarboxylic acid cycle intermediates, 20 free fatty acids, and three bile acids in rat kidney tissue. A differential spatial distribution of endogenous carboxyl-containing metabolites was shown in the kidney. Higher ion intensities of tricarboxylic acid cycle intermediates were detected in the renal medulla and pelvis, whereas free fatty acids showed higher levels in the renal cortex. Bile acids were essentially distributed throughout the inner cortex of the kidney. They also carried out simultaneous MALDI MSI of free fatty acids and phospholipids in rat brain sections to better understand the complex metabolic pathways of this organ. Their results showed phosphatidylcholine and lysophosphatidylcholine to be mainly located in the cerebral cortex and thalamus of rat brain and free fatty acids to present much stronger ion intensities in the cerebral cortex, amygdala, and hippocampus.

7. Targeted chemical function: Double bond group

a. Benzaldehyde

Benzaldehyde is a new Paternò Büchi reagent that reacts in a [2+2] cycloaddition (Table 7a). Bednařík *et al.*⁶⁰ used benzaldehyde, a reagent compatible with MALDI MSI to localize carbon-carbon double bonds of unsaturated phospho- and glycolipids. Indeed, the differential double-bond location of unsaturated phospholipids offers a better understanding of isomer-specific functions and metabolism.⁶¹ The authors also used MALDI-2 to enhance the protonation yield of Paternò Büchi compounds. Derivatization was performed on mouse brain sections and followed by CID to generate characteristic ion pairs that reveal the double bond position. This strategy showed differential localization of several phosphatidylcholine and phosphatidylserine double-bond positional isomers in the white and the gray matter of the cerebellum (Figure 3).

b. Benzophenone +hν

Benzophenone reacts with phospholipids in a [2+2] Paternò Büchi reaction upon UV laser (343 nm) irradiation during the MALDI process (Table 7b). Benzophenone is the first reactive matrix inducing a derivatization reaction during the MALDI process. Wäldchen *et al.*⁶² used benzophenone for the determination of double-bond positional isomers. CID of Paternò Büchi product ions results in formation of two fragment ions for every DB-position in a retro-Paternò Büchi reaction. They were thus able to localize double-bond positional isomers in mouse cerebellum sections at a high lateral resolution, down to 15 μm. Additionally, they applied their workflow to study the unknown surface distribution of phospholipids in the parasite *Schistosoma mansoni*.

c. Ozone

Ozone reacts with double bonds to form ozonides (Table 7c). Paine *et al.*⁶³ introduced the ozone-induced dissociation reactions to MALDI MSI. Ozone-induced dissociation is a versatile method that allows the authors to resolve both double bond-positional isomers of lipids and *sn*-positional isomers (esterification position of fatty acyl chains). Thus, they introduced ozone in a linear ion-trap mass spectrometer which enabled the visualization of multiple isomeric lipids in different regions of the rat brain. Bednařík *et al.*⁶⁴ introduced an off-line on-tissue ozonation protocol that allowed the derivatization of unsaturated phospholipids in tissue sections. The use of gaseous ozone under dry conditions for the derivatization of phospholipids in tissue sections minimizes the risk of delocalization. They applied the developed

ozonation technique with MS² on derivatized phospholipids formed called Criegee ozonide. They demonstrated that PC 34:1 Δ 9 isomer was more abundant in white matter of mouse brain than the Δ 11 isomer (lipid nomenclature explained in the reference⁶⁴). The ozonation protocol was also applied to human colon and revealed different ratios of PC 34:1 Δ 11 to PC 34:1 Δ 9 isomers, ranging from 0.1 to 0.5 in colon muscle, mucosa, and mucosa-associated lymphatic tissue, respectively.

8. Targeted chemical function: Phosphate monoester group

a. Phos-tag (zinc complex)

Despite recent advances in MALDI MSI, it is still difficult, in some cases, to detect low abundant phospholipids in tissues. Iwama *et al.*⁶⁵ developed a novel OTCD using a zinc complex, the Phos-tag, that reacts with phosphate monoester group (Table 8). After OTCD, they were able to visualize minor bioactive lipids such as lysophosphatidic acid and sphingosine-1-phosphate within murine brain by MALDI MSI. Other phosphate monoester containing lipids were also detected after Phos-tag derivatization such as phosphatidic acid and ceramide-1-phosphate.

9. Other targeted functions

a. Derivatization of Diene group of Vitamine D Metabolites with Ampiflex

Ampiflex reacts with Diene group of Vitamin D and its metabolites in a Diels-Alder reaction (Table 9). Vitamin D is a steroid-class compound mainly formed through UV exposure of the skin. It is an essential component for numerous biological processes, such as immune functions⁶⁶ and calcium homeostasis⁶⁷. It is studied not only in the context of vitamin-D deficiency but also as a potential treatment for cancer and mental disorders.⁶⁸ Vitamin D is first metabolized to 25-hydroxyvitamin D (25-(OH)-D) in the liver and is a clinical biomarker. It is then metabolized to 1 α ,25-dihydroxyvitamin D (1,25-(OH)₂-D) in the kidney.⁶⁹ Vitamin-D metabolites are measured in biological matrices by LC-MS/MS after chemical derivatization because of their lack of ionizable moieties. Therefore, Smith *et al.*⁶⁸ developed an OTCD method for the detection of vitamin-D metabolites in murine kidney tissue by MSI. They used MALDI and DESI MSI to evaluate three different derivatization reagents: Ampiflex, 4-phenyl-1,2,4-triazoline-3,5-dione (PTAD), and 4-(2-(6,7-Dimethoxy-4-methyl-3-oxo-3,4-dihydroquinoxaliny)ethyl)-1,2,4-triazoline-3,5-dione (DMEQ-TAD). Ampiflex vitamin-D

derivatives showed good ionization without analyte diffusion within the tissue in MALDI relative to DESI MSI. Vitamin-D metabolites were then detected in murine kidney, where the precursor 25-(OH)-D undergoes a second hydroxylation and produces 1,25-(OH)₂-D. They detected 1,25-(OH)₂-D₃ essentially in the cortex near the renal vein, whereas 25-(OH)-D₃ was mainly distributed across the medulla and inner cortex, the formation of its metabolite being depth dependent. 3D molecular mapping analysis may thus provide valuable information about the metabolism of vitamin D throughout the tissue.

b. Derivatization of Platinum compounds with DDTC

The diethyldithiocarbamate (DDTC) is a nucleophilic sulfur containing compound that forms metallic complexes by chelating with metallic ions such as Pt(II), Pt(IV) and others (Table 10). The distribution of platinum-based drugs, which are commonly used for cancer treatment, is of interest, but their distribution in tumor tissues is unknown, as techniques for their detection suffer from low sensitivity. Consequently, Liu *et al.*⁷⁰ developed an OTCD method using DDTC, which forms an ionizable complex with the platinum-based drug. 3D multicellular tumor spheroid *in vitro* models were used in this study. In addition, they combined the MSI results and UPLC-MRM of derivatized drugs to quantify them. This method was applied to oxaliplatin and its metabolites (cisplatin and carboplatin) to localize and quantify them in the tumor spheroids and optimize hyperthermic intraperitoneal chemotherapy.

c. Derivatization of 3-MoSA with TCDI

Chacon *et al.*⁷¹ used the 1,1'-thiocarbonyldiimidazole (TCDI) derivatization reagent to map the 3-methoxysalicylamine (3-MoSA), a scavenger of Levuglandins (LGs) in tissues. The derivatization reaction resulted in an oxazine derivative (Table 11), improving the sensitivity of 3-MoSA detection. The 3-MoSA prevents the formation of LG adducts, which are linked to oxidative injury, inflammation, and progression of Alzheimer's disease when present at high levels. OTCD with TCDI revealed the spatial distribution of the drug in various organs of mice treated with 3-MoSA, such as the kidneys. In addition, the average signal intensity of 3-MoSA-TCDI (normalized to that of the TIC) showed a clear trend of clearance of the drug. This trend was consistent with the results obtained during previous quantification experiments using LC-ESI-MS/MS.

d. Derivatization of sialic acid in glycans by EDC

Holst *et al.*⁷² applied an OTCD procedure using a modified version of dimethylamidation for the stabilization of sialic acid (Table 12). They developed an OTCD protocol that improves the detection of sialylated N-glycans and differentiates them from various N-glycans. The protocol was applied on formalin-fixed and paraffin-embedded human colon carcinoma and leiomyosarcoma tissues. Indeed, glycans are involved in numerous molecular and biological processes that occur during cancer progression, such as immune modulation and metastasis formation, cell-matrix interactions, and cell communication.⁷³ In addition, glycans are potential biomarkers and treatment targets. However, their analysis by MALDI MSI is challenging because of the presence of sialic acid leading to salt adduct formation, the negative charge of their carboxylic acid, and their labile character. The authors applied 1-ethyl-3-(3-dimethylamino)propyl carbodiimide (EDC) as a carboxylic acid activator and 1-hydroxybenzotriazole (HOBt) as a catalyst for the derivatization reaction with a modified version of dimethylamidation. They also introduced an additional step using ammonia to hydrolyze lactones formed after the first step because of their instability. This strategy allowed the stabilization of the sialic acid without lateral diffusion, which made the mapping of N-glycans possible in FFPE tissues.

e. Derivatization of the reducing terminus of N-Glycans by GirP

The hydrazine group of GirP reacts with the reducing terminus of glycans to yield a GirP-glycan conjugate (Table 13). Recently, Zhang *et al.*⁷⁴ developed an OTCD protocol using GirP reagent for the analysis of N-glycans from FFPE-treated tissue sections. The approach was evaluated by the analysis of monosaccharides, oligosaccharides, and N-glycans released from glycoproteins after treatment with the PNGase F enzyme. Derivatization using GirP reagent enhanced the signals by 230-fold for glucose and 28-fold for maltooctaose, with a notable increase of the S/N ratios. An improvement coverage of the glycome was obtained for N-glycans released from bovine thyroglobulin and human immunoglobulin G after derivatization. Moreover, OTCD was applied to human laryngeal cancer (Figure 4) and ovarian cancer tissues. The results showed differential expression of N-glycans between normal and cancer tissue regions. Higher expression of high-mannose type N-glycans was detected in the tumor regions after derivatization. Such N-glycans could serve as promising candidates for cancer biomarkers after further studies.

10. Multi-OTCD

The combination of OTCD reactions that target different chemical functions enables the visualization of several classes of compounds. Dueñas *et al.*⁷⁵ carried out a proof-of-concept experiment, in which several classes of compounds containing amine, carboxylic acid, and carbonyl groups were targeted by different derivatization reagents. They selected coniferyl aldehyde for primary amines (Table 1b), the GirT reagent for carbonyl groups (Table 4a), and 2-picolylamine for carboxylic acids (Table 6a). The combination of these three derivatization reagents allowed the visualization of various classes of compounds in an untargeted manner. This approach was applied to leaves and root sections from two different maize genotypes (B73 and Mo17) and allowed the detection of over 600 new unique metabolites, demonstrating that OTCD has potential for untargeted metabolomic-scale studies.

Guo *et al.*⁷⁶ combined laser-assisted tissue transfer technique with CA (Table 1b) derivatization for amine containing metabolites and GirT derivatization for steroids (Table 4a). This technique enabled the imaging of 67 amino-metabolites such as neurotransmitters, amino acids, dipeptides and different steroids such as dehydrocorticosterone and corticosterone in rat brain tissue sections.

Takeo *et al.*⁷⁷ employed OTCD using GirT for ketone-containing steroid molecules (Table 412a) and TAHS for amine-containing catecholamine molecules (Table 1a). For steroid detection, they employed MS³ that made it possible to distinguish the mineralocorticoid aldosterone and a glucocorticoid cortisol from their structural isomers. It was also useful for the detection of hybrid steroids, such as 18-hydroxycortisol and 18-oxocortisol. MS³ allows the discrimination between steroids and their isomers after their derivatization because it produces specific ion transitions for different GirT-derivatized steroids. They applied this method to confirm the differences between the distribution of aldosterone in adrenal tissues of control rats and those subjected to a sodium-deficient diet. In addition, they evaluated the clinical applicability of OTCD coupled to tandem MSI by measuring cortisol, aldosterone, and 18-hydroxycortisol levels in human adrenal glands. They identified the presence of small aldosterone-producing cell clusters that produced high level of aldosterone in clinical specimens but that did not contain cortisol. They extend their study to derivatize catecholamine by TAHS reagent coupled to tandem MSI for the detection of catecholamine species in pathological adrenal gland tissues from patients. Indeed, there are two types of pheochromocytoma tumors, those that secrete adrenalin and those that secrete noradrenalin, depending on the cell

type. The authors demonstrated the efficiency of OTCD to discriminate between the two types of pheochromocytoma tumor by visualizing the levels of adrenaline and noradrenaline in tissues.

Conclusion and perspectives

MSI is a powerful analytical tool for monitoring the distribution of large arrays of molecules within tissues in different application fields including biology, pharmacology, toxicology, etc. There is thus a strong need to improve the sensitivity of this technique to address numerous biological questions. Here, we reviewed various applications in which OTCD was successfully used for the improvement of the detection of molecules bearing different chemical functions but also for the differentiation of isomers, the stabilization of molecules, and their structural characterization (Figure 5). The development of new methods of OTCD should be a focus of ongoing MALDI MSI research. In addition, the transfer of derivatization methods intensively used in ESI⁷⁸ to MALDI MSI and the further optimization of protocols that already exist could result in new beneficial protocols. As shown in this review, OTCD is mainly applied to small exogenous and endogenous molecules. Efforts are needed to extend this method to larger molecules such as peptides⁷⁹ and oligonucleotides⁸⁰ in order to enhance their ionization yield or to allow the orientation of the fragmentation toward specific series of fragment ions which simplify their identification as shown by Franck *et al.*⁴³

Novel technologies introduced in the field of MALDI MSI such as MALDI-2, are not available for all users. OTCD offers a simple and low-cost method and remains a solution of choice for many MS users. On the other hand, when available, the combination of MALDI-2 and OTCD can present a great potential for significantly improve sensitivity and selectivity. Other aspects of sample preparation could also be used and developed such as tissue washing protocols that enable the reduction of untargeted species which decreases the signal extinction.⁸¹ The introduction of new matrices could also solve the problem of the sensitivity of certain molecules by generating appropriate matrix-analyte complexes for ionization by MALDI.⁸² The low sensitivity of MALDI MSI has long been a challenge. The continuous development on sample preparation and novel technologies to improve sensitivity in this field will lead to larger applicability thus allowing a better understanding of biological mechanisms and diseases.

References

- [1] R. M. Caprioli, T. B. Farmer, J. Gile. Molecular imaging of biological samples: Localization of peptides and proteins using MALDI-TOF MS. *Anal Chem.* **1997**, *69*, 4751.
- [2] B. Chatterji, A. Pich. MALDI imaging mass spectrometry and analysis of endogenous peptides. *Expert Rev Proteomics.* **2013**, *10*, 381.
- [3] E. Astigarraga, G. Barreda-Gomez, L. Lombardero, O. Fresnedo, F. Castano, M. T. Giralt, B. Ochoa, R. Rodriguez-Puertas, J. A. Fernandez. Profiling and imaging of lipids on brain and liver tissue by matrix-assisted laser desorption/ ionization mass spectrometry using 2-mercaptobenzothiazole as a matrix. *Anal Chem.* **2008**, *80*, 9105.
- [4] R. R. Drake, C. A. West, A. S. Mehta, P. M. Angel. MALDI Mass Spectrometry Imaging of N-Linked Glycans in Tissues. *Adv Exp Med Biol.* **2018**, *1104*, 59.
- [5] M. Stoeckli, P. Chaurand, D. E. Hallahan, R. M. Caprioli. Imaging mass spectrometry: A new technology for the analysis of protein expression in mammalian tissues. *Nat Med.* **2001**, *7*, 493.
- [6] B. Prideaux, M. Stoeckli. Mass spectrometry imaging for drug distribution studies. *J Proteomics.* **2012**, *75*, 4999.
- [7] S. Schulz, M. Becker, M. R. Groseclose, S. Schadt, C. Hopf. Advanced MALDI mass spectrometry imaging in pharmaceutical research and drug development. *Current Opinion in Biotechnology.* **2019**, *55*, 51.
- [8] J. Quanco, J. Franck, M. Wisztorski, M. Salzet, I. Fournier. Progress and Potential of Imaging Mass Spectrometry Applied to Biomarker Discovery. *Methods Mol Biol.* **2017**, *1598*, 21.
- [9] Y. Yoshimura, N. Goto-Inoue, T. Moriyama, N. Zaima. Significant advancement of mass spectrometry imaging for food chemistry. *Food Chem.* **2016**, *210*, 200.
- [10] K. Susniak, M. Krysa, B. Gieroba, I. Komaniecka, A. Sroka-Bartnicka. Recent developments of MALDI MSI application in plant tissues analysis. *Acta Biochim Pol.* **2020**, *67*, 277.
- [11] R. Bradshaw, G. Wilson, N. Denison, S. Francese. Application of MALDI MS imaging after sequential processing of latent fingerprints. *Forensic Sci Int.* **2021**, *319*, 110643.

- [12] F. Tobias, A. B. Hummon. Considerations for MALDI-Based Quantitative Mass Spectrometry Imaging Studies. *Journal of Proteome Research*. **2020**, *19*, 3620.
- [13] T. Porta, A. Lesur, E. Varesio, G. Hopfgartner. Quantification in MALDI-MS imaging: what can we learn from MALDI-selected reaction monitoring and what can we expect for imaging? *Anal Bioanal Chem*. **2015**, *407*, 2177.
- [14] D. Mesa Sanchez, S. Creger, V. Singla, R. T. Kurulugama, J. Fjeldsted, J. Laskin. Ion Mobility-Mass Spectrometry Imaging Workflow. *Journal of the American Society for Mass Spectrometry*. **2020**, *31*, 2437.
- [15] M. Niehaus, J. Soltwisch, M. E. Belov, K. Dreisewerd. Transmission-mode MALDI-2 mass spectrometry imaging of cells and tissues at subcellular resolution. *Nat Methods*. **2019**, *16*, 925.
- [16] E. C. Spivey, J. C. McMillen, D. J. Ryan, J. M. Spraggins, R. M. Caprioli. Combining MALDI-2 and transmission geometry laser optics to achieve high sensitivity for ultra-high spatial resolution surface analysis. *J Mass Spectrom*. **2019**, *54*, 366.
- [17] T. Santa. Derivatization in liquid chromatography for mass spectrometric detection. *Drug Discov Ther*. **2013**, *7*, 9.
- [18] K. Shimbo, A. Yahashi, K. Hirayama, M. Nakazawa, H. Miyano. Multifunctional and Highly Sensitive Precolumn Reagents for Amino Acids in Liquid Chromatography/Tandem Mass Spectrometry. *Anal Chem*. **2009**, *81*, 5172.
- [19] S. Toue, Y. Sugiura, A. Kubo, M. Ohmura, S. Karakawa, T. Mizukoshi, J. Yoneda, H. Miyano, Y. Noguchi, T. Kobayashi, Y. Kabe, M. Suematsu. Microscopic imaging mass spectrometry assisted by on-tissue chemical derivatization for visualizing multiple amino acids in human colon cancer xenografts. *Proteomics*. **2014**, *14*, 810.
- [20] M. Arts, Z. Soons, S. R. Ellis, K. A. Pierzchalski, B. Balluff, G. B. Eijkel, L. J. Dubois, N. G. Lieuwes, S. M. Agten, T. M. Hackeng, van Loon, Luc J. C., R. M. A. Heeren, Olde Damink, Steven W. M. Detection of Localized Hepatocellular Amino Acid Kinetics by using Mass Spectrometry Imaging of Stable Isotopes. *Angew Chem Int Ed Engl*. **2017**, *56*, 7146.
- [21] J. Wappler, M. Arts, A. Röth, R. M.A. Heeren, U. Peter Neumann, S. W. Olde Damink, Z. Soons, T. Cramer. Glutamine deprivation counteracts hypoxia-induced chemoresistance. *Neoplasia*. **2020**, *22*, 22.

- [22] M. L. Manier, M. L. Reyzer, A. Goh, V. Dartois, L. E. Via, C. E. 3. Barry, R. M. Caprioli. Reagent precoated targets for rapid in-tissue derivatization of the anti-tuberculosis drug isoniazid followed by MALDI imaging mass spectrometry. *Journal of the American Society for Mass Spectrometry*. **2011**, *22*, 1409.
- [23] M. L. Manier, J. M. Spraggins, M. L. Reyzer, J. L. Norris, R. M. Caprioli. A derivatization and validation strategy for determining the spatial localization of endogenous amine metabolites in tissues using MALDI imaging mass spectrometry. *J Mass Spectrom*. **2014**, *49*, 665.
- [24] Y. Enomoto, P. Nt An, M. Yamaguchi, E. Fukusaki, S. Shimma. Mass Spectrometric Imaging of GABA in the *Drosophila melanogaster* Adult Head. *Anal Sci*. **2018**, *34*, 1055.
- [25] L. Qin, Y. Zhang, Y. Liu, H. He, M. Han, Y. Li, M. Zeng, X. Wang. Recent advances in matrix-assisted laser desorption/ionisation mass spectrometry imaging (MALDI-MSI) for in situ analysis of endogenous molecules in plants. *Phytochem Anal*. **2018**, *29*, 351.
- [26] K. C. O'Neill, Y. J. Lee. Visualizing Genotypic and Developmental Differences of Free Amino Acids in Maize Roots With Mass Spectrometry Imaging. *Front Plant Sci*. **2020**, *11*, 639.
- [27] M. Dilillo, R. Ait-Belkacem, C. Esteve, D. Pellegrini, S. Nicolardi, M. Costa, E. Vannini, E. L. d. Graaf, M. Caleo, L. A. McDonnell. Ultra-High Mass Resolution MALDI Imaging Mass Spectrometry of Proteins and Metabolites in a Mouse Model of Glioblastoma. *Sci Rep*. **2017**, *7*, 603.
- [28] F. Eto, S. Sato, M. Setou, I. Yao. Region-specific effects of Scrapper on the abundance of glutamate and gamma-aminobutyric acid in the mouse brain. *Sci Rep*. **2020**, *10*, 7435.
- [29] F. Eto, S. Sato, M. Setou, I. Yao, K. Sato. Mass spectrometry imaging reveals glycine distribution in the developing and adult mouse brain. *J Chem Neuroanat*. **2020**, *110*, 101869.
- [30] E. Sugiyama, M. M. Guerrini, K. Honda, Y. Hattori, M. Abe, P. Källback, P. E. Andrén, K. F. Tanaka, M. Setou, S. Fagarasan, M. Suematsu, Y. Sugiura. Detection of a High-Turnover Serotonin Circuit in the Mouse Brain Using Mass Spectrometry Imaging. *iScience*. **2019**, *20*, 359.
- [31] E. Sugiyama, T. Kondo, N. Kuzumaki, K. Honda, A. Yamanaka, M. Narita, M. Suematsu, Y. Sugiura. Mechanical allodynia induced by optogenetic sensory nerve excita-

tion activates dopamine signaling and metabolism in medial nucleus accumbens. *Neurochem Int.* **2019**, *129*, 104494.

- [32] Q. Cao, Y. Wang, B. Chen, F. Ma, L. Hao, G. Li, C. Ouyang, L. Li. Visualization and Identification of Neurotransmitters in Crustacean Brain via Multifaceted Mass Spectrometric Approaches. *ACS Chem Neurosci.* **2019**, *10*, 1222.
- [33] M. Shariatgorji, A. Nilsson, P. Kallback, O. Karlsson, X. Zhang, P. Svenningsson, P. E. Andren. Pyrylium Salts as Reactive Matrices for MALDI-MS Imaging of Biologically Active Primary Amines. *Journal of the American Society for Mass Spectrometry.* **2015**, *26*, 934.
- [34] M. Shariatgorji, A. Nilsson, R. J. A. Goodwin, P. Kallback, N. Schintu, X. Zhang, A. R. Crossman, E. Bezdard, P. Svenningsson, P. E. Andren. Direct targeted quantitative molecular imaging of neurotransmitters in brain tissue sections. *Neuron.* **2014**, *84*, 697.
- [35] R. Shariatgorji, A. Nilsson, N. Strittmatter, T. Vallianatou, X. Zhang, P. Svenningsson, R. J. A. Goodwin, P. E. Andren. Bromopyrylium derivatization facilitates identification by mass spectrometry imaging of monoamine neurotransmitters and small molecule neuroactive compounds. *Journal of the American Society for Mass Spectrometry.* **2020**.
- [36] Z. Takáts, J. M. Wiseman, B. Gologan, R. G. Cooks. Mass spectrometry sampling under ambient conditions with desorption electrospray ionization. *Science.* **2004**, *306*, 471.
- [37] C. Harkin, K. W. Smith, F. L. Cruickshank, C. Logan Mackay, B. Flinders, R. M. A. Heeren, T. Moore, S. Brockbank, D. F. Cobice. On-tissue chemical derivatization in mass spectrometry imaging. *Mass Spectrom Rev.* **2021**, *n/a*.
- [38] C. Esteve, E. A. Tolner, R. Shyti, A. M. J. M. van den Maagdenberg, L. A. McDonnell. Mass spectrometry imaging of amino neurotransmitters: A comparison of derivatization methods and application in mouse brain tissue. *Metabolomics.* **2016**, *12*, 30.
- [39] M. Shariatgorji, A. Nilsson, E. Fridjonsdottir, T. Vallianatou, P. Kallback, L. Katan, J. Savmarker, I. Mantas, X. Zhang, E. Bezdard, P. Svenningsson, L. R. Odell, P. E. Andren. Comprehensive mapping of neurotransmitter networks by MALDI-MS imaging. *Nat Methods.* **2019**, *16*, 1021.
- [40] X. Zhang, I. Mantas, E. Fridjonsdottir, P. E. Andrén, K. Chergui, P. Svenningsson. Deficits in Motor Performance, Neurotransmitters and Synaptic Plasticity in Elderly and Ex-

perimental Parkinsonian Mice Lacking GPR37. *Frontiers in Aging Neuroscience*. **2020**, *12*, 84.

[41] G. Li, F. Ma, Q. Cao, Z. Zheng, K. DeLaney, R. Liu, L. Li. Nanosecond photochemically promoted click chemistry for enhanced neuropeptide visualization and rapid protein labeling. *Nature Communications*. **2019**, *10*, 4697.

[42] T. Ito, M. Hiramoto. Use of mTRAQ derivatization reagents on tissues for imaging neurotransmitters by MALDI imaging mass spectrometry: the triple spray method. *Anal Bioanal Chem*. **2019**, *411*, 6847.

[43] J. Franck, M. El Ayed, M. Wisztorski, M. Salzet, I. Fournier. On-tissue N-terminal peptide derivatizations for enhancing protein identification in MALDI mass spectrometric imaging strategies. *Anal Chem*. **2009**, *81*, 8305.

[44] E. Beasley, S. Francese, T. Bassindale. Detection and Mapping of Cannabinoids in Single Hair Samples through Rapid Derivatization and Matrix-Assisted Laser Desorption Ionization Mass Spectrometry. *Anal Chem*. **2016**, *88*, 10328.

[45] I. Kaya, S. M. Brulls, J. Dunevall, E. Jennische, S. Lange, J. Martensson, A. G. Ewing, P. Malmberg, J. S. Fletcher. On-Tissue Chemical Derivatization of Catecholamines Using 4-(N-Methyl)pyridinium Boronic Acid for ToF-SIMS and LDI-ToF Mass Spectrometry Imaging. *Anal Chem*. **2018**, *90*, 13580.

[46] T. T. Forsman, M. E. Dueñas, Y. J. Lee. On-tissue boronic acid derivatization for the analysis of vicinal diol metabolites in maize with MALDI-MS imaging. *J Mass Spectrom*. **2021**, *56*, e4709.

[47] D. F. Cobice, C. L. Mackay, R. J. A. Goodwin, A. McBride, P. R. Langridge-Smith, S. P. Webster, B. R. Walker, R. Andrew. Mass spectrometry imaging for dissecting steroid intracrinology within target tissues. *Anal Chem*. **2013**, *85*, 11576.

[48] D. F. Cobice, D. E. W. Livingstone, A. McBride, C. L. MacKay, B. R. Walker, S. P. Webster, R. Andrew. Quantification of 11 β -hydroxysteroid dehydrogenase 1 kinetics and pharmacodynamic effects of inhibitors in brain using mass spectrometry imaging and stable-isotope tracers in mice. *Biochem Pharmacol*. **2018**, *148*, 88.

[49] D. F. Cobice, D. E. W. Livingstone, C. L. Mackay, R. J. A. Goodwin, L. B. Smith, B. R. Walker, R. Andrew. Spatial Localization and Quantitation of Androgens in Mouse Testis by Mass Spectrometry Imaging. *Anal Chem*. **2016**, *88*, 10362.

- [50] S. Shimma, H.-O. Kumada, H. Taniguchi, A. Konno, I. Yao, K. Furuta, T. Matsuda, S. Ito. Microscopic visualization of testosterone in mouse testis by use of imaging mass spectrometry. *Anal Bioanal Chem.* **2016**, *408*, 7607.
- [51] F. P. Y. Barre, B. Flinders, J. P. Garcia, I. Jansen, L. R. S. Huizing, T. Porta, L. B. Creemers, R. M. A. Heeren, B. Cillero-Pastor. Derivatization Strategies for the Detection of Triamcinolone Acetonide in Cartilage by Using Matrix-Assisted Laser Desorption/Ionization Mass Spectrometry Imaging. *Anal Chem.* **2016**, *88*, 12051.
- [52] Y. Sugiura, E. Takeo, S. Shimma, M. Yokota, T. Higashi, T. Seki, Y. Mizuno, M. Oya, T. Kosaka, M. Omura, T. Nishikawa, M. Suematsu, K. Nishimoto. Aldosterone and 18-Oxocortisol Coaccumulation in Aldosterone-Producing Lesions. *Hypertension.* **2018**, *72*, 1345.
- [53] H. Enomoto, T. Senu, E. Yumoto, T. Yokota, H. Yamane. Derivatization for detection of abscisic acid and 12-oxo-phytodienoic acid using matrix-assisted laser desorption/ionization imaging mass spectrometry. *Rapid Commun Mass Spectrom.* **2018**, *32*, 1565.
- [54] E. Yutuc, R. Angelini, M. Baumert, N. Mast, I. Pikuleva, J. Newton, M. R. Clench, D. O. F. Skibinski, O. W. Howell, Y. Wang, W. J. Griffiths. Localization of sterols and oxysterols in mouse brain reveals distinct spatial cholesterol metabolism. *Proc Natl Acad Sci U S A.* **2020**, *117*, 5749.
- [55] B. Flinders, J. Morrell, P. S. Marshall, L. E. Ranshaw, M. R. Clench. The use of hydrazine-based derivatization reagents for improved sensitivity and detection of carbonyl containing compounds using MALDI-MSI. *Anal Bioanal Chem.* **2015**, *407*, 2085.
- [56] A. Fülöp, T. Bausbacher, S. Rizzo, Q. Zhou, H. Gillandt, C. Hopf, M. Rittner. New Derivatization Reagent for Detection of free Thiol-groups in Metabolites and Proteins in Matrix-Assisted Laser Desorption/Ionization Mass Spectrometry Imaging. *Anal Chem.* **2020**, *92*, 6224.
- [57] Q. Wu, T. J. Comi, B. Li, S. S. Rubakhin, J. V. Sweedler. On-Tissue Derivatization via Electrospray Deposition for Matrix-Assisted Laser Desorption/Ionization Mass Spectrometry Imaging of Endogenous Fatty Acids in Rat Brain Tissues. *Anal Chem.* **2016**, *88*, 5988.

- [58] S.-S. Wang, Y.-J. Wang, J. Zhang, T.-Q. Sun, Y.-L. Guo. Derivatization Strategy for Simultaneous Molecular Imaging of Phospholipids and Low-Abundance Free Fatty Acids in Thyroid Cancer Tissue Sections. *Anal Chem.* **2019**, *91*, 4070.
- [59] C. Sun, W. Liu, Y. Geng, X. Wang. On-Tissue Derivatization Strategy for Mass Spectrometry Imaging of Carboxyl-Containing Metabolites in Biological Tissues. *Anal Chem.* **2020**, *92*, 12126.
- [60] A. Bednarik, S. Bolsker, J. Soltwisch, K. Dreisewerd. An On-Tissue Paterno-Buchi Reaction for Localization of Carbon-Carbon Double Bonds in Phospholipids and Glycolipids by Matrix-Assisted Laser-Desorption-Ionization Mass-Spectrometry Imaging. *Angew Chem Int Ed Engl.* **2018**, *57*, 12092.
- [61] T. Hu, J.-L. Zhang. Mass-spectrometry-based lipidomics. *J Sep Sci.* **2018**, *41*, 351.
- [62] F. Waldchen, B. Spengler, S. Heiles. Reactive Matrix-Assisted Laser Desorption/Ionization Mass Spectrometry Imaging Using an Intrinsically Photoreactive Paterno-Buchi Matrix for Double-Bond Localization in Isomeric Phospholipids. *J Am Chem Soc.* **2019**, *141*, 11816.
- [63] M. R. L. Paine, B. L. J. Poad, G. B. Eijkel, D. L. Marshall, S. J. Blanksby, R. M. A. Heeren, S. R. Ellis. Mass Spectrometry Imaging with Isomeric Resolution Enabled by Ozone-Induced Dissociation. *Angew Chem Int Ed Engl.* **2018**, *57*, 10530.
- [64] A. Bednařík, J. Preisler, D. Bezdeková, M. Machálková, M. Hendrych, J. Navrátilová, L. Knopfová, E. Moskovets, J. Soltwisch, K. Dreisewerd. Ozonization of Tissue Sections for MALDI MS Imaging of Carbon-Carbon Double Bond Positional Isomers of Phospholipids. *Anal Chem.* **2020**, *92*, 6245.
- [65] T. Iwama, K. Kano, D. Saigusa, K. Ekroos, G. van Echten-Deckert, J. Vogt, J. Aoki. Development of an On-Tissue Derivatization Method for MALDI Mass Spectrometry Imaging of Bioactive Lipids Containing Phosphate Monoester Using Phos-tag. *Anal Chem.* **2021**.
- [66] R. Nair, A. Maseeh. Vitamin D: The "sunshine" vitamin. *Journal of pharmacology & pharmacotherapeutics.* **2012**, *3*, 118.
- [67] J. C. Fleet. The role of vitamin D in the endocrinology controlling calcium homeostasis. *Mol Cell Endocrinol.* **2017**, *453*, 36.

- [68] K. W. Smith, B. Flinders, P. D. Thompson, F. L. Cruickshank, C. L. Mackay, R. M. A. Heeren, D. F. Cobice. Spatial Localization of Vitamin D Metabolites in Mouse Kidney by Mass Spectrometry Imaging. *ACS Omega*. **2020**, *5*, 13430.
- [69] D. D. Bikle. Vitamin D metabolism, mechanism of action, and clinical applications. *Chem Biol*. **2014**, *21*, 319.
- [70] X. Liu, A. B. Hummon. Chemical Imaging of Platinum-Based Drugs and their Metabolites. *Sci Rep*. **2016**, *6*, 38507.
- [71] A. Chacon, I. Zagol-Ikapitte, V. Amarnath, M. L. Reyzer, J. A. Oates, R. M. Caprioli, O. Boutaud. On-tissue chemical derivatization of 3-methoxysalicylamine for MALDI-imaging mass spectrometry. *J Mass Spectrom*. **2011**, *46*, 840.
- [72] S. Holst, B. Heijs, N. de Haan, R. J. M. van Zeijl, I. H. Briaire-de Bruijn, G. W. van Pelt, A. S. Mehta, P. M. Angel, W. E. Mesker, R. A. Tollenaar, R. R. Drake, J. V. M. G. Bovee, L. A. McDonnell, M. Wuhrer. Linkage-Specific in Situ Sialic Acid Derivatization for N-Glycan Mass Spectrometry Imaging of Formalin-Fixed Paraffin-Embedded Tissues. *Anal Chem*. **2016**, *88*, 5904.
- [73] S. S. Pinho, C. A. Reis. Glycosylation in cancer: mechanisms and clinical implications. *Nature Reviews Cancer*. **2015**, *15*, 540.
- [74] H. Zhang, X. Shi, N. Q. Vu, G. Li, Z. Li, Y. Shi, M. Li, B. Wang, N. V. Welham, M. S. Patankar, P. Weisman, L. Li. On-Tissue Derivatization with Girard's Reagent P Enhances N-Glycan Signals for Formalin-Fixed Paraffin-Embedded Tissue Sections in MALDI Mass Spectrometry Imaging. *Anal Chem*. **2020**, *92*, 13361.
- [75] M. E. Duenas, E. A. Larson, Y. J. Lee. Toward Mass Spectrometry Imaging in the Metabolomics Scale: Increasing Metabolic Coverage Through Multiple On-Tissue Chemical Modifications. *Front Plant Sci*. **2019**, *10*, 860.
- [76] S. Guo, W. Tang, Y. Hu, Y. Chen, A. Gordon, B. Li, P. Li. Enhancement of On-tissue Chemical Derivatization by Laser-Assisted Tissue Transfer for MALDI MS Imaging. *Anal Chem*. **2019**, *92*, 1431.
- [77] E. Takeo, Y. Sugiura, T. Uemura, K. Nishimoto, M. Yasuda, E. Sugiyama, S. Ohtsuki, T. Higashi, T. Nishikawa, M. Suematsu, E. Fukusaki, S. Shimma. Tandem Mass Spectrometry Imaging Reveals Distinct Accumulation Patterns of Steroid Structural Isomers in Human Adrenal Glands. *Anal Chem*. **2019**, *91*, 8918.

- [78] Y. Iwasaki, Y. Nakano, K. Mochizuki, M. Nomoto, Y. Takahashi, R. Ito, K. Saito, H. Nakazawa. A new strategy for ionization enhancement by derivatization for mass spectrometry. *J Chromatogr B Analyt Technol Biomed Life Sci.* **2011**, 879, 1159.
- [79] B. Beine, H. C. Diehl, H. E. Meyer, C. Henkel. Tissue MALDI Mass Spectrometry Imaging (MALDI MSI) of Peptides. *Methods Mol Biol.* **2016**, 1394, 129.
- [80] Y. Nakashima, M. Setou. Distribution of Antisense Oligonucleotides in Rat Eyeballs Using MALDI Imaging Mass Spectrometry. *Mass Spectrom (Tokyo).* **2018**, 7, A0070-A0070.
- [81] H. Yang, W. Ji, M. Guan, S. Li, Y. Zhang, Z. Zhao, L. Mao. Organic washes of tissue sections for comprehensive analysis of small molecule metabolites by MALDI MS imaging of rat brain following status epilepticus. *Metabolomics.* **2018**, 14, 50.
- [82] C. D. Calvano, A. Monopoli, T. R. I. Cataldi, F. Palmisano. MALDI matrices for low molecular weight compounds: An endless story? *Anal Bioanal Chem.* **2018**, 410, 4015.

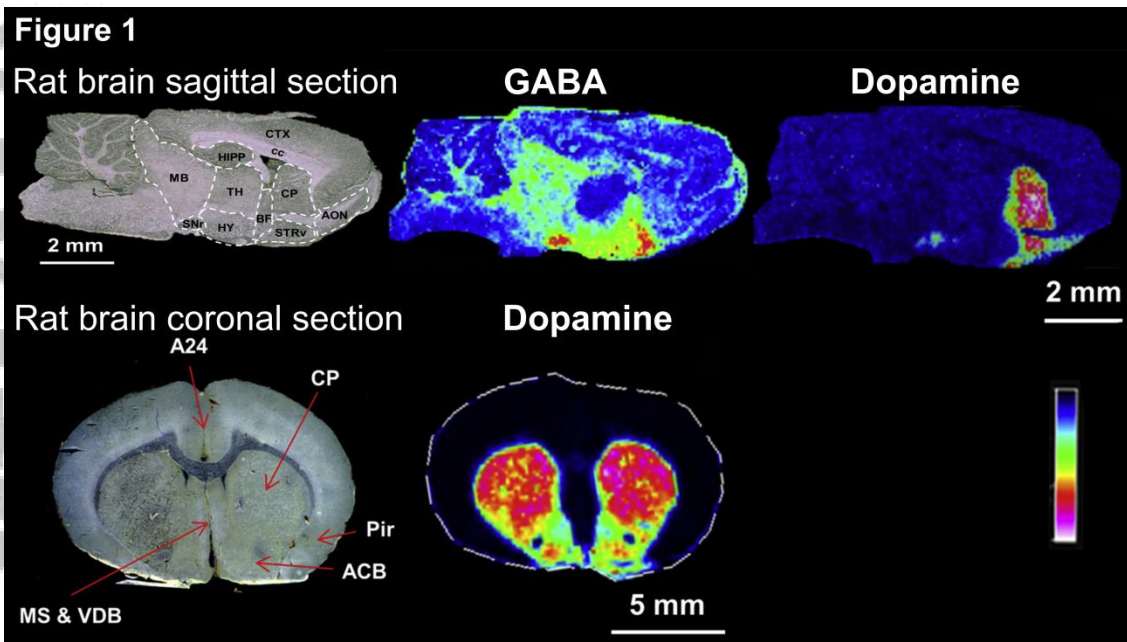


Figure 1. OTCD of primary amine functions in neurotransmitters by the DPP-TFB derivatization reagent. OTCD revealed the distribution of GABA and dopamine in sagittal and coronal rat brain sections at a lateral resolution of 100 μm and 150 μm , respectively. Abbreviations: substantia nigra (SN), caudate-putamen (CP), ventral striatum (STRv), anterior olfactory nucleus (AON), cingulate cortex (area 24) (A24), piriform cortex (Pir), medial septal nucleus (MS), nucleus of the vertical limb of the diagonal band (VDB), accumbens nucleus (ACB), hypothalamus (HY), thalamus (TH), hippocampus (HIPP), corpus callosum (cc), cerebral cortex (CTX), midbrain (MB), basal forebrain (BF). Adapted from Shariatgorji *et al.*³⁴ with permission.

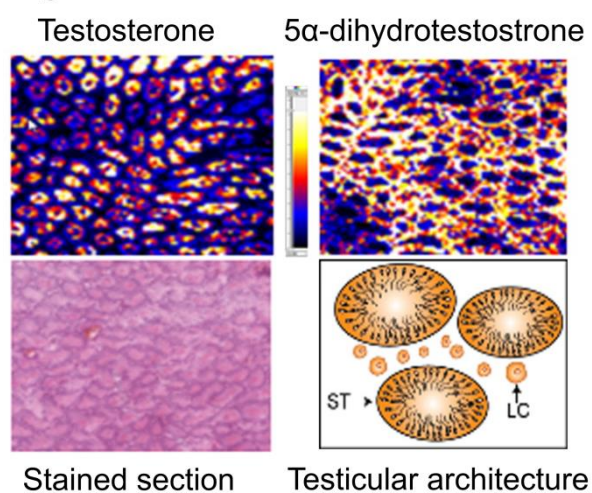
Figure 2

Figure 2. OTCD of ketone functions in steroids using the GirT reagent. Distribution of testosterone and 5 α -dihydrotestosterone in the testis of mice stimulated with human chorionic gonadotrophin at a lateral resolution of 50 μ m. Abbreviations: seminiferous tubule (ST), Leydig cells (LC). Adapted from Cobice *et al.*⁴⁹ with permission.

Figure 3

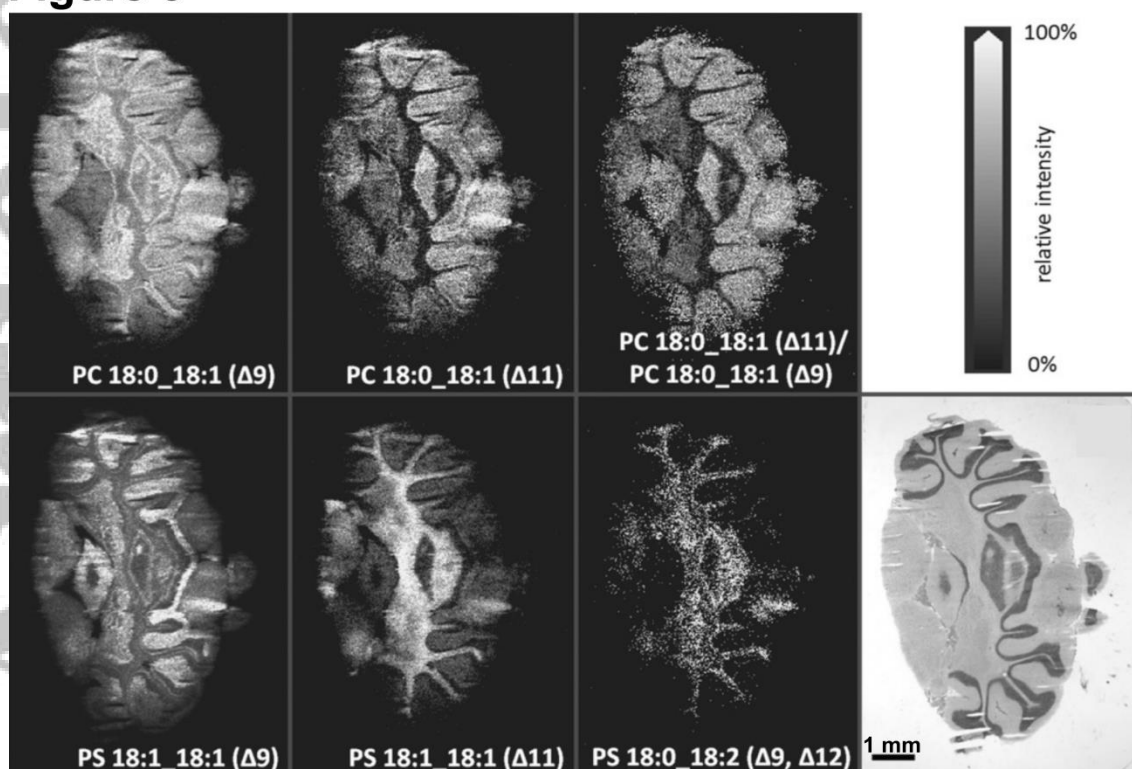


Figure 3. Distinction of double-bond positional isomers of phosphatidylcholines (PC) and phosphatidylserines (PS) using the benzaldehyde derivatization reagent combined with MALDI-2 analysis. Isomers were differentiated by MALDI MSI experiments performed in the MS/MS mode. Distribution of the PC 18:0_18:1($\Delta 9$) and PC 18:0_18:1($\Delta 11$) isomers and the PS 18:1_18:1($\Delta 9$), PS 18:1_18:1($\Delta 11$), and PS 18:0_18:2 ($\Delta 9, \Delta 12$) isomers in mouse brain sections. Adapted from Bednařík *et al.*⁶⁰ with permission.

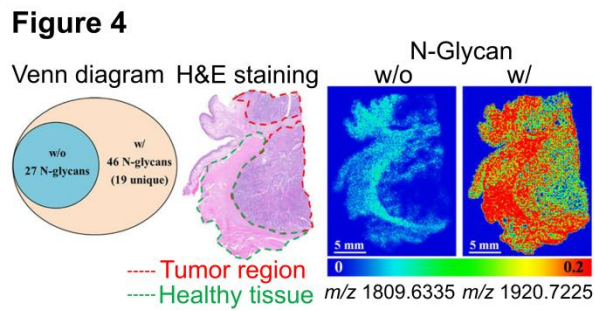


Figure 4. Enhancement of N-glycans after OTCD with the GirP reagent applied to human laryngeal cancer tissue section. The Venn diagram showed the improved number of N-glycans detected without (w/o) and with (w/) OTCD. MALDI images of ions detected at m/z 1809.6335 and m/z 1920.7225 corresponded to Hex5HexNAc4dHex1 w/o or w/ respectively. Adapted from Zhang *et al.*⁷⁴ with permission.

Figure 5

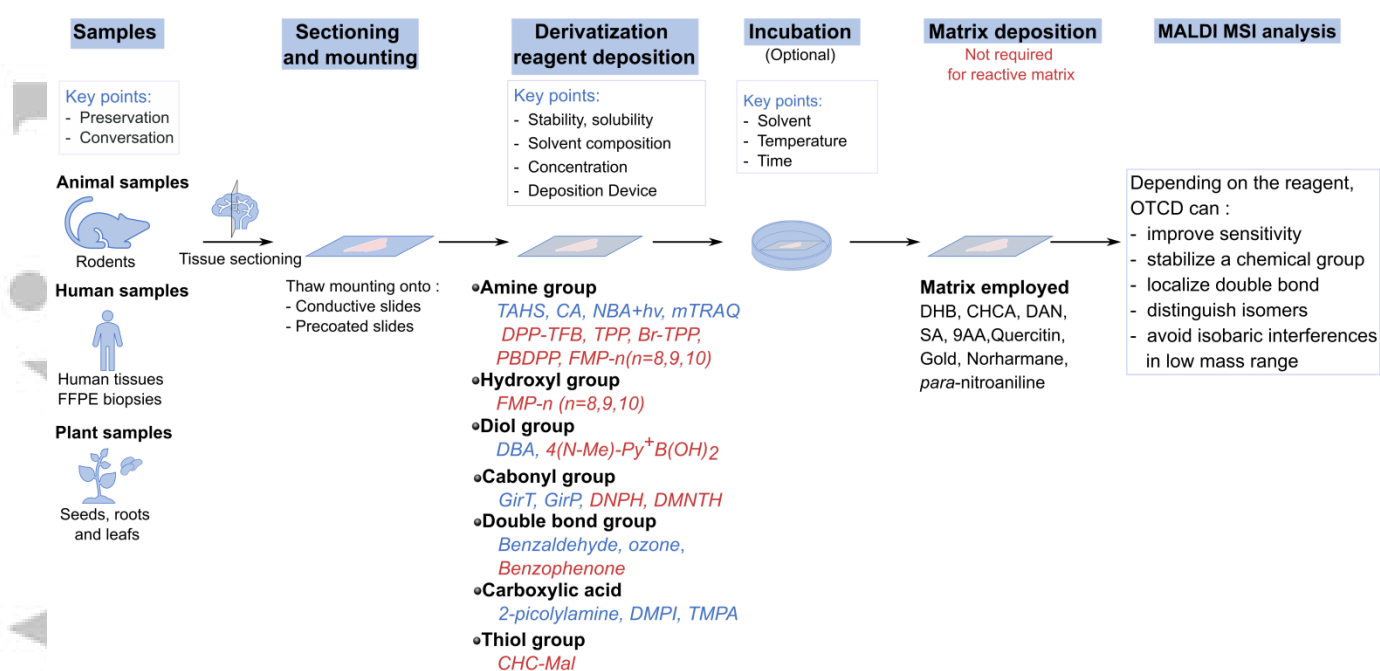
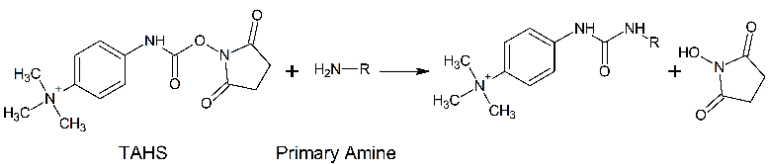


Figure 5. Scheme representing the different steps of an OTCD protocol for MALDI MSI analysis and the key points. Samples and derivatization reagents correspond to those cited in this review.

Accepted

Table 1. OTCD targeting amine function

Primary Amine						
a. Reaction with TAHS						
 <p style="text-align: center;"> TAHS Primary Amine </p>						
Analyte	OTCD protocol			Matrix	Sample	Ref.
	Solution of derivatization reagent	Application method	Incubation or other treatment			
Alanine, glutamate, glutamine, glycine, leucine/isoleucine/hydroxyproline, phenylalanine, proline, tryptophan, tyrosine, etc.	5 mg/mL in ACN	Airbrush deposition	overnight at 55 °C	DHB 20mg/mL (ACN +0.2 % formate)	Liver tissues from xenograft mouse models of human colon cancer	Toue <i>et al.</i> ¹⁹
Phenylalanine, Tyrosine	5 mg/mL in ACN	Automatic spraying	24 h at 55 °C in humid environment (50% MeOH /H2O)	DHB 30 mg/mL (70% MeOH + 0.2% TFA)	Liver tissues from xenograft mouse model of H460 human NSCLC	Arts <i>et al.</i> ²⁰

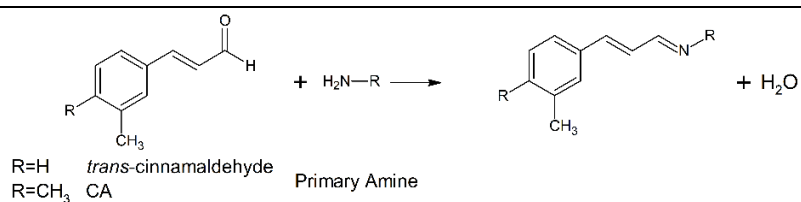
a. Reaction with TAHS (*continued*)

Analyte	OTCD protocol			Matrix	Sample	Ref.
	Solution of derivatization reagent	Application method	Incubation or other treatment			
Glutamine	5 mg/mL in ACN	Automatic spraying	24 h at 55 °C in a humid environment (50% MeOH /H ₂ O)	DHB 30 mg/ mL (70% MeOH + 0.2% TFA)	Tumor tissues from patients with cholangiocarcinoma	Wappler <i>et al.</i> ²¹
Adrenaline, Noradrenaline	5 mg/mL ACN	Airbrush deposition	15 min at 55 °C	DHB 50 mg/ mL (ACN)	Adrenal gland tissues from tumor patients and from rats fed with (normal sodium) or (deficient sodium) diet	Takeo <i>et al.</i> ⁷⁷

a. Reaction with TAHS (continued)

Analyte	OTCD protocol			Matrix	Sample	Ref.
	Solution of derivatization reagent	Application method	Incubation or other treatment			
3-methoxytyramine, Alanine, aspartate, dopamine, GABA, glutamate, glutamine, glycine, L-dihydroxyphenylalanine, leucine/isoleucine, lysine, phenylalanine, proline, serine, taurine, threonine, tryptophan, tyrosine, valine	5 mg/mL in 50 % ACN	Automatic spraying	overnight at 55 °C	DHB 30 mg/ mL (70% MeOH + 0.1% TFA)	Brain tissues from female C57BL/6J mice	Esteve <i>et al.</i> ³⁸

b. Reaction with Cinnamaldehydes (continued)



Analyte	OTCD Protocol			Matrix	Sample	Ref.
	Solution of derivatization reagent	Application method	Incubation or other treatment			
Isoniazid	<i>Trans</i> -cinnamaldehyde in 50% MeOH (precoated slide)	High velocity spin coating	30 min at room temperature	CHCA 15 mg/mL (60% ACN + 0.1% TFA) (sprayer)	Lung tissues from rabbits infected with tuberculosis and dosed with isoniazid	Manier <i>et al.</i> ²²
Dopamine, epinephrine, GABA, norepinephrine	CA 23 mg/ml + 8.5 mg/mL <i>trans</i> -ferulic acid in MeOH (precoated slide)	Automatic Sprayer	-	8.5 mg/ml <i>trans</i> -ferulic acid in MeOH (mixed and sprayed with the derivatization reagent)	Pig adrenal gland, rat cerebellum	Manier <i>et al.</i> ²³

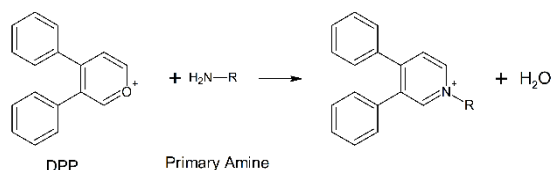
b. Reaction with Cinnamaldehydes (continued)

Analyte	OTCD Protocol			Matrix	Sample	Ref.
	Solution of derivatization reagent	Application method	Incubation or other treatment			
GABA	CA 11.5 mg/ml of CA + 4.25 mg of trans-FA in MeOH	Airbrush deposition	10 min at room temperature	CHCA 10 mg/mL in 30% ACN, 10% 2-propanol and 0.1% formic acid after sublimation deposition first-step	Head tissue from wild type strain and female of <i>Drosophila melanogaster</i>	Enomoto <i>et al.</i> ²⁴
67 amine-containing metabolites (amino acids, neurotransmitters, dipeptides and others)	CA 5 mg/mL in 50% MeOH	Electrospray deposition	Overnight at 37 °C in a humid environment	DHB 30 mg/mL in 50% MeOH / Quercetin 5 mg/mL in 80% MeOH	Brain tissues from Sprague-Dawley rat	Guo <i>et al.</i> ⁷⁶

b. Reaction with Cinnamaldehydes (continued)

Analyte	OTCD Protocol			Matrix	Sample	Ref.
	Solution of derivatization reagent	Application method	Incubation or other treatment			
Alanine, GABA, glycine, isoleucine/leucine, serine, threonine, valine, etc.	CA 20 mg/mL in MeOH	Automatic Spraying	Spraying of 6.5 mM of Potassium acetate	Gold (sputter coating)	Maize root tissues	O Neil <i>et al.</i> ²⁶
Alanine, aminobutenoic acid, GABA, Glycine, Leucine/isoleucine, Serine, etc.	CA 20 mg/mL in MeOH	Automatic Spraying or electrospray deposition	Spraying of 6.5 mM of Potassium acetate	Gold or DHB 40 mg/mL (70% MeOH) or DAN 20 mg/mL DAN	Leaf and root sections from two different maize genotypes (B73 and Mo17)	Dueñas <i>et al.</i> ⁷⁵

c. Reaction with DPP-TFB (continued)



Analyte	OTCD Protocol			Matrix	Sample	Ref.
	Solution of derivatization reagent	Application method	Incubation or other treatment			
3-methoxytyramine, alanine, aspartate, dopamine, GABA, glutamate, glutamine, glycine, leucine, L-dihydroxyphenylalanine, lysine, proline, serotonin, taurine, threonine, tryptophan, tyramine, tyrosine, valine	DPP-TFB 5 mg/mL in MeOH	Automatic Spraying	Overnight incubation	DHB 30 mg/mL in 70% MeOH + 0.1 % TFA	Brain tissue sections from glioblastoma multiforme and WT mice	Dilillo <i>et al.</i> ²⁷
GABA, glutamate	DPP-TFB 1.33 mg/mL in MeOH	Manual Spraying	-	DHB 40 mg/mL in 50% MeOH (automatic Sprayer)	Brain tissue from Scrapper KO and WT mice	Eto <i>et al.</i> ²⁸

c. Reaction with DPP-TFB (<i>continued</i>)						
Analyte	OTCD Protocol			Matrix	Sample	Ref.
	Solution of derivatization reagent	Application method	Incubation or other treatment			
Glycine	DPP-TFB 1.33 mg/mL in MeOH	Manual Spraying	-	DHB 40 mg/mL in 50% MeOH (automatic Sprayer)	Brain tissues from 5-day-old and 8-week-old (adult) male mice	Eto <i>et al.</i> ²⁹
Dopamine, norepinephrine, serotonin	DPP-TFB 1.3 mg/mL in MeOH	Manual Spraying	-	DHB 40 mg/mL in 50% MeOH (automatic Sprayer)	Brain tissues from C57BL/6J male mice	Sugiyama <i>et al.</i> ³⁰
3-methoxytyramine, dopamine	DPP-TFB 1.3 mg/mL in MeOH	Manual Spraying	-	DHB 40 mg/mL in 50% MeOH (automatic Sprayer)	Brain tissues from C57BL/6J male mice	Sugiyama <i>et al.</i> ³¹
Dopamine, GABA, histamine, serotonin	DPP-TFB 1.33 mg/mL in 75% MeOH + 0.05% TEA	Automatic spraying	24 hours at room temperature	DHB 40 mg/mL in MeOH/H ₂ O/FA 49.95/49.95/0.1)	Brain tissues from Rock crabs <i>Cancer irroratus</i>	Cao <i>et al.</i> ³²

c. Reaction with DPP-TFB (continued)

Analyte	OTCD Protocol			Matrix	Sample	Ref.
	Solution of derivatization reagent	Application method	Incubation or other treatment			
GABA	DPP-TFB 0.79 mg/mL in 60% MeOH + 1.3 % TEA	Airbrush deposition	60 min incubation in MeOH vapor saturated chamber then spraying of 10% acetic acid solution	CHCA 10 mg/mL in 30% ACN, 10% 2-propanol + 0.1% FA after sublimation deposition first-step	Head tissue from wild type strain of <i>Drosophila melanogaster</i> and female <i>Drosophila melanogaster</i>	Enomoto <i>et al.</i> ²⁴
Amphetamine, dopamine, β -N-methylamino-L-alanine	DPP 1.11 mg/mL in 75% MeOH + 0.05% TEA PBDPP 0.2 mg/mL in 80% MeOH + 0.07% TEA	Automatic spraying	15 min incubation in MeOH vapor saturated chamber	DPP and PBDPP as reactive matrices	Brain tissues from Sprague–Dawley rats, male Wistar rat pups, and C57BL/6J male mice with and without treatment	Shariatgorji <i>et al.</i> ³³
	TMP 1 mg/mL in 83% MeOH + 0.05% TEA DPP 1.11 mg/mL in 75% MeOH + 0.05% TEA	Automatic spraying	15 min incubation in MeOH vapor saturated chamber (+ drying by nitrogen)	CHCA 5 mg/mL in 50% ACN +0.2% TFA		

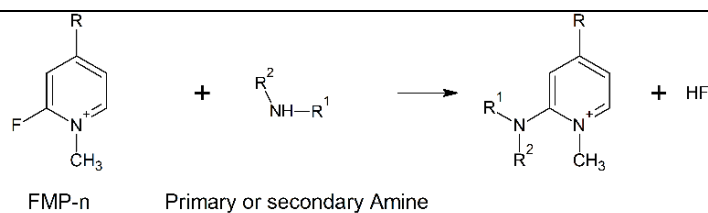
c. Reaction with DPP-TFB (continued)

Analyte	OTCD Protocol			Matrix	Sample	Ref.
	Solution of derivatization reagent	Application method	Incubation or other treatment			
3-methoxytyramine, dopamine, GABA, glutamate, phenethylamine, serotonin, tryptamine, tyramine, Tyrosine	DPP-TFB / TMP-TFB 0.091 mg/mL in 50% MeOH + 0.067% TEA	Automatic spraying	60 min incubation in MeOH vapor saturated chamber, then spraying of acetic acid/H ₂ O/MeOH (10/45/45) solution, then 30 min incubation in MeOH vapor saturated chamber	CHCA 5 mg/mL or 10 mg/mL in 50% ACN + 0.2% TFA	Brain tissues from Sprague-Dawley rats, C57BL/6J male mice and primate with and without treatment	Shariatgorji <i>et al.</i> ³⁴
	DPP-TFB 1.34 mg/mL in 70% MeOH + 0.049 % TEA	Automatic spraying	15 min incubation in MeOH vapor saturated chamber (+ drying by nitrogen flow every 5 min)	DPP-TFB as reactive matrix		

c. Reaction with DPP-TFB (continued)

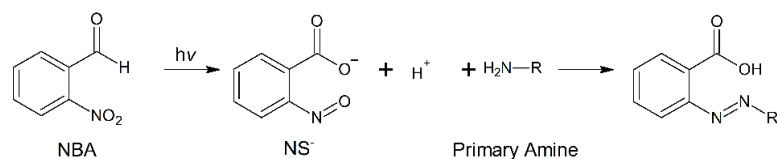
Analyte	OTCD Protocol			Matrix	Sample	Ref.
	Solution of derivatization reagent	Application method	Incubation or other treatment			
Dopamine, fluvoxamine, GABA	TPP and Br-TPP 1.3 mg/mL in 80% MeOH + 0.058 % TEA	Automatic Spraying	15 min incubation in MeOH vapor saturated chamber (+ drying by nitrogen flow every 5 min)	TPP and Br-TPP as Reactive matrices	Brain tissues from Sprague–Dawley rats and C57BL/6J male mice	Shariatgorji <i>et al.</i> ³⁵
3-methoxytyramine, alanine, aspartate, dopamine, GABA, glutamate, glutamine, glycine, leucine/isoleucine, L- dihydroxyphenylalanine, lysine, proline, serine, seroto- nin, taurine, threonine, trypto- phan, valine	DPP-TFB 5 mg/mL in MeOH	Automatic Spraying	Overnight at room temperature	DHB 30 mg/ mL in 70% MeOH + 0.1% TFA	Brain tissues from female C57BL/6J mice	Esteve <i>et al.</i> ³⁸

d. Reaction with FMP-n (continued)



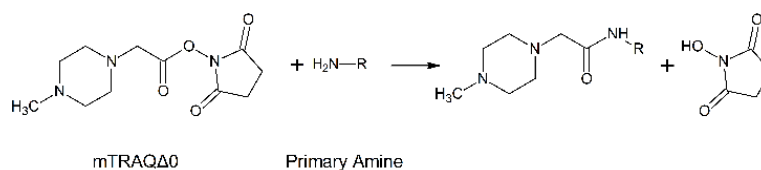
Analyte	OTCD Protocol			Matrix	Sample	Ref.
	Solution of derivatization reagent	Application method	Incubation or other treatment			
Major neurotransmitters, including their metabolites, of the dopaminergic and serotonergic systems containing primary and secondary amine groups	FMP-8, FMP-9, FMP-10 at 4.4 mM in 70% ACN	Automatic Spraying	-	FMP-8, FMP-9 and FMP-10 as reactive matrices	Brain tissues from rat and primate models of Parkinson's disease and from a patient with Parkinson's disease	Shariatgorji <i>et al.</i> ³⁹
Dopamine, GABA	FMP-10 at 1.8 mg/mL in 70% ACN	Automatic Spraying	-	FMP-10 as reactive matrix	Brain tissues from GPR37 KO and WT mice	Zhang <i>et al.</i> ⁴⁰

e. Reaction with NBA+hv (continued)



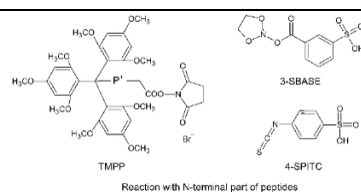
Analyte	OTCD Protocol			Matrix	Sample	Ref.
	Solution of derivatization reagent	Application method	Incubation or other treatment			
Neuropeptides	5 mg/mL in ACN/EtOH/FA/H ₂ O (84/13/0.3/2.7)	Automatic Spraying	Nanosecond laser irradiation	CHCA 5 mg/mL in ACN/H ₂ O/FA (49.95/49.95/0.1) for peptides and small proteins. SA 20 mg/mL in ACN/H ₂ O/FA (49.95:49.95:0.1) for larger proteins analysis	Brain tissues from mouse	Li <i>et al.</i> ⁴¹

f. Reaction with mTRAQ (continued)



Analyte	OTCD Protocol			Matrix	Sample	Ref.
	Solution of derivatization reagent	Application method	Incubation or other treatment			
GABA	20 μL of mTRAQΔ0 in 45% ACN and 55% H ₂ O	Automatic Spraying	1 hour at 32°C in humid environment	DHB 30 mg/mL in 70% EtOH + 0.1% TFA	Brain tissues from male WKY and SHRSP rats	Ito <i>et al.</i> ⁴²

g. Reaction with TMPP, 3S-BASE and 4-SPITC (continued)



Analyte	OTCD Protocol			Matrix	Sample	Ref.
	Solution of derivatization reagent	Application method	Incubation or other treatment			
Peptides	4-SPITC 10 mg/mL in 25 mM NH ₄ HCO ₃ buffer	Manual Spotting	1 h at 50 °C (MeOH/H ₂ O environment) Then deposition of 1% TFA	For proteins imaging: ionic matrix solution: containing 10 mg/mL of SA and 8.1 μL of aniline in 0.1% ACN/TFA (6.4, v/v) For peptides imaging: ionic matrix solution: containing 10 mg/mL of CHCA and 7.2 μL of aniline in 0.1% ACN/TFA (6:4, v/v)	Brain tissues from rat	Franck <i>et al.</i> ⁴³
	3-SBASE 20 mg/mL in 25 mM NH ₄ HCO ₃ buffer	Manual spotting and automatic microspotting	1 h at 50 °C (MeOH/H ₂ O environment) Then deposition of 1% TFA			
	TMPP 1 mg/mL in 30 % ACN	Manual spotting and automatic microspotting	Deposition of 1% TEA (in ACN/H ₂ O) Then incubation for 1h at room temperature			

NSCLC (non-small cell lung carcinoma), *TEA* (triethylamine), *TFA* (Trifluoroacetic acid), *FA* (formic acid), *KO* (Knock-out), *WT* (wild type), γ -aminobutyric (*GABA*), *sinapic acid* (*SA*).

Table 2. OTCD targeting phenol function

Hydroxyl group						
Reaction with FMP-n						
<p style="text-align: center;"> <chem>CN1C=CC(F)=C1.Rc1ccc(O)cc1>>Rc1ccc(Oc2cc(C)nc(F)c2)cc1.F</chem> </p> <p style="text-align: center;"> FMP-n Phenolic hydroxyl </p>						
Analyte	OTCD Protocol			Matrix	Sample	Ref.
	Solution of derivatization reagent	Application method	Incubation or other treatment			
Neurotransmitters, including their metabolites, of the dopaminergic and serotonergic systems containing phenolic hydroxyl groups	FMP-8, FMP-9, FMP-10 at 4.4 mM in 70% ACN	Automatic Spraying	-	FMP-8, FMP-9 and FMP-10 as reactive matrices	Brain tissues from rat and primate models of Parkinson's disease and from a patient with Parkinson's disease	Shariatgotji <i>et al.</i> ³⁹
Cannabinoids and their metabolites	FMPTS 10 mg/mL in ACN	Airbrush deposition	-	CHCA 5 mg/mL in 70% ACN +0.2% TFA (automatic sprayer)	Human Hair	Beasley <i>et al.</i> ⁴⁴

Table 3. OTCD targeting diol function

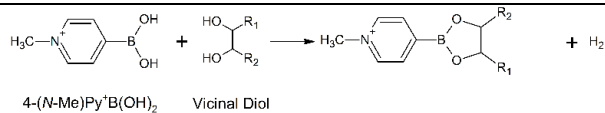
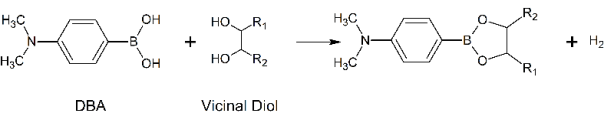
Diol group						
Reaction with Boronic acid						
 <p style="text-align: center;">4-(N-Me)Py⁺B(OH)₂ Vicinal Diol</p>						
 <p style="text-align: center;">DBA Vicinal Diol</p>						
Analyte	OTCD Protocol			Matrix	Sample	Ref.
	Solution of derivatization reagent	Application method	Incubation or other treatment			
Catecholamines (dopamine, epinephrine, and norepinephrine)	4-(N-Me)Py ⁺ B(OH) ₂ 12 mg/mL in 60% ACN	Automatic spraying	-	4-(N-Me)Py ⁺ B(OH) ₂ as reactive matrix	Porcine adrenal gland tissue sections	Kaya <i>et al.</i> ⁴⁵
Vicinal diol containing molecules (glycosides, lipopolysaccharides, monosaccharides, and many other metabolites)	DBA 50 mM in MeOH	Automatic Spraying	-	Silver DHB 40 mg/mL in MeOH/H ₂ O 70/30 CHCA 10 mg/mL in ACN/H ₂ O 70/30 +0.1% TFA DAN 10 mg/mL in ACN/H ₂ O	B73 maize stems, roots and leaves	Forsman <i>et al.</i> ⁴⁶

Table 4. OTCD targeting carbonyl function

Carbonyl group						
a. Reaction with GirT						
<p style="text-align: center;"> Girard T Carbonyl </p>						
Analyte	OTCD Protocol			Matrix	Sample	Ref.
	Solution of derivatization reagent	Application method	Incubation or other treatment			
11-dehydrocorticosterone, Corticosterone	0.15 mg/cm ²	Precoated slide	Spraying of MeOH + 0.2% TFA then 60 min incubation at 40°C in a humid environment then allowed to cool in a vacuum desiccator for 15 min at room temperature	CHCA 10 mg/mL in 80% ACN + 0.2% TFA	Tissue sections from adrenal gland of Sprague-Dawley male rat and from brain of C57BL/6 male mice	Cobice <i>et al.</i> ⁴⁷

a. Reaction with GirT (continued)

Analyte	OTCD Protocol			Matrix	Sample	Ref.
	Solution of derivatization reagent	Application method	Incubation or other treatment			
Deuterated Cortisol, corticosterone, cortisone	5 mg/mL in MeOH 80% + 0.1%TFA	Manually	60 min incubation at 40 °C and 80% relative humidity then allowed to cool in vacuum desiccator for 15 min at room temperature	CHCA 10 mg/mL in 80% ACN + 0.2% TFA	Brain tissues from treated and untreated C57BL/6 mice and mice with genetic disruption <i>Hsd11b1</i>	Cobice <i>et al.</i> ⁴⁸
5 α -dihydrotestosterone, testosterone	5 mg/mL in MeOH 80% + 0.1%TFA	Airbrush deposition and automatic spraying for higher resolution)	60 min incubation at 40 °C and 80% relative humidity then allowed to cool in vacuum desiccator for 15 min at room temperature	CHCA 10 mg/mL in 80% ACN + 0.2% TFA	Testis tissues from C57BL/6 male mice prostate tissues from male Sprague-Daley rats treated with human chorionic gonadotrophin	Cobice <i>et al.</i> ⁴⁹

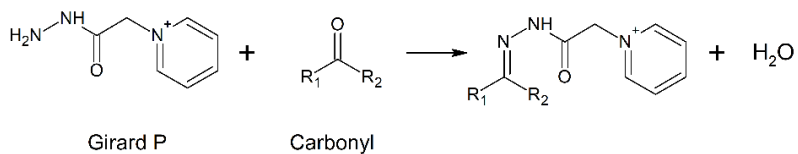
a. Reaction with GirT (continued)

Analyte	OTCD Protocol			Matrix	Sample	Ref.
	Solution of derivatization reagent	Application method	Incubation or other treatment			
Testosterone	5 mg/mL in 2.5% acetic acid	Airbrush deposition	90 min at room temperature	Two-step matrix application. 1) Sublimation 2) Spraying: CHCA 10 mg/mL in ACN/Isopropanol/H ₂ O (3/1/6) + 0.1% FA	Testis tissues from from C57BL/6 male mice treated with human chorionic gonadotrophin	Shimma <i>et al.</i> ⁵⁰
Triamcinolone acetonide	5 mg/mL in MeOH + 0.2% TFA	Automatic spraying	150 min at 40°C	DHB 20 mg/mL in 70% MEOH + 0.2% TFA	Cartilage tissues from patients	Barré <i>et al.</i> ⁵¹
18-oxocortisol, 18-hydroxycortisol aldosterone, cortisol, cortisone, progesterone	10 mg/mL in 20% acetic acid	Airbrush deposition	90 min at room temperature	FT-ICR-MS analysis: DHB in 80% EtOH + saturated ammonium sulfate (50 mg/mL) Tandem MS analysis: Two-step matrix application. 1) Sublimation 2) Spraying: CHCA 10 mg/mL in ACN/Isopropanol/H ₂ O (3/1/6) + 0.1% FA	Adrenal gland tissues from patients and Sprague-Dawley male rats	Sugiura <i>et al.</i> ⁵²

a. Reaction with GirT (continued)

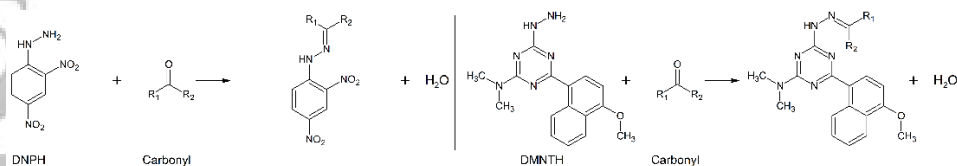
Analyte	OTCD Protocol			Matrix	Sample	Ref.
	Solution of derivatization reagent	Application method	Incubation or other treatment			
12-oxo-phytodienoic acid, abscisic acid	5 mg/mL in 80% MeOH + 2% TFA	Airbrush deposition	30 min at room temperature then allowed to dry in vacuum desiccator for 30 min	DHB 40 mg/mL in 70% MeOH + 0.1% FA	Sections from <i>Phaseolus vulgaris L</i> seeds	Enomoto <i>et al.</i>
18-hydroxycortisol, 18-oxocortisol, aldosterone, cortisol, cortisone	10 mg/mL in 20% acetic acid	Airbrush deposition	60 min at room temperature	Two-step matrix application. 1) Sublimation 2) Spraying: CHCA 10 mg/mL in ACN/Isopropanol/H ₂ O (3/1/6) + 0.1% FA	Adrenal gland tissues from patients and Sprague-Dawley male rats	Takeo <i>et al.</i> ⁷⁷
1-hexanal, 1-heptanal, jasmonic acid, pyruvic acid, and others	10 mg/mL in MeOH + 2% TFA	Automatic Spraying or electrospray deposition	Spraying of 6.5 mM of Potassium acetate	Gold or DHB 40 mg/mL (70% MeOH) or DAN 20 mg/mL DAN	Leaf and root sections from two different maize genotypes (B73 and Mo17)	Dueñas <i>et al.</i> ⁷⁵
11-dehydrocorticosterone, corticosterone, dexamethasone	5 mg/mL in 80% MEOH + 0.2% TFA	Electrospray deposition	1 h at 40°C in a humid environment	DHB 30 mg/mL in 50 % MeOH / Quercetin 5 mg/mL in 80% MeOH	Brain tissues from Sprague-Dawley rat	Guo <i>et al.</i> ⁷⁶

b. Reaction with GirP (continued)



Analyte	OTCD Protocol			Matrix	Sample	Ref.
	Solution of derivatization reagent	Application method	Incubation or other treatment			
Cholestenic acids, oxysterols, sterols	5 mg/mL in 70% MeOH + 5% acetic acid (after deposition of cholesterol oxidase)	Automatic spraying	1 h at 37°C in water bath then allowed to dry in a vacuum desiccator	CHCA 5 mg/mL in H ₂ O/propan-2-ol/ACN (3/4/3)	Brain tissues from wild type and cholesterol 24S-hydroxylase knockout mice	Yutuc <i>et al.</i> ⁵⁴

c. Reaction with DNPH and DMNTH (continued)



Analyte	OTCD Protocol			Matrix	Sample	Ref.
	Solution of derivatization reagent	Application method	Incubation or other treatment			
Fluticasone propionate	DNPH: 4 mg/mL in 50% ACN + 0.1% TFA	Spotting	-	DNPH as reactive matrix	Lung tissues from rats	Flinders <i>et al.</i> ⁵⁵
	DMNTH: 5 mg/mL in 50% ACN + 0.1% TFA		48 h at 37°C in a humid environment with 5% carbon dioxide	DMNTH as reactive matrix		

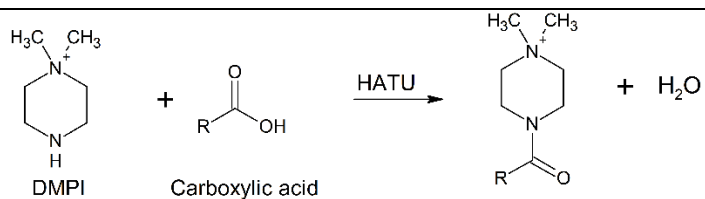
Table 5.OTCD targeting thiol function

Thiol group						
Reaction with CHC-Mal						
<p style="text-align: center;">CHC-Mal + HS-R → Thiol</p>						
Analyte	OTCD Protocol			Matrix	Sample	Ref.
	Solution of derivatization reagent	Application method	Incubation or other treatment			
α and β chains of reduced insulin, cysteine, cysteinylglycine, glutathione	10 mg/mL in 50% ACN	Automatic spraying	-	CHC-Mal as reactive matrix for small thiol-containing metabolites DHB 60 mg/mL in 50% ACN for protein measurements	Liver and pancreas tissues from pig, tumor tissues from mouse xenograft	Fülöp <i>et al.</i> ⁵⁶

Table 6. OTCD targeting carboxylic acid function

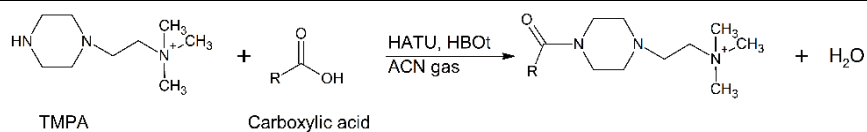
Carboxylic acid group						
a. Reaction with 2-picolyamine						
<p style="text-align: center;"> 2-picolyamine Carboxylic acid </p>						
Analyte	OTCD Protocol			Matrix	Sample	Ref.
	Solution of derivatization reagent	Application method	Incubation or other treatment			
Arachidonic acid, docosahexaenoic acid, eicosapentaenoic acid, linolenic acid, oleic acid, palmitic acid, palmitoleic acid, stearic acid	2 mM of 2-picolyamine + 10 mM of TPP and DPDS in ACN	Electrospraying or airbrush deposition	-	9-AA or DHB by sublimation	Brain tissues from Sprague-Dawley rats	Wu <i>et al.</i> ⁵⁷
Oleic acid, palmitic acid, stearic acid and others	6 mM of 2-picolyamine + 30 mM of TPP and DPDS in ACN	Automatic Spraying or electrospray deposition	Spraying of 6.5 mM of Potassium acetate	Gold or DHB 40 mg/mL (70% MeOH) or DAN 20 mg/mL DAN	Leaf and root sections from two different maize genotypes (B73 and Mo17)	Dueñas <i>et al.</i> ⁷⁵

b. Reaction with DMPI (continued)



Analyte	OTCD Protocol			Matrix	Sample	Ref.
	Solution of derivatization reagent	Application method	Incubation or other treatment			
Free fatty acids (C16:0 and C18:0 and many others)	DMPI 3 mM and HATU at 1mM in 80% ACN	Electrospray deposition	-	DHB 25 mg/mL in 80% MeOH + 0.2% TFA	Carcinoma and para-carcinoma tissues from patients with thyroid carcinoma and rat brain tissues.	Wang <i>et al.</i> ⁵⁸

c. Reaction with TMPA (continued)

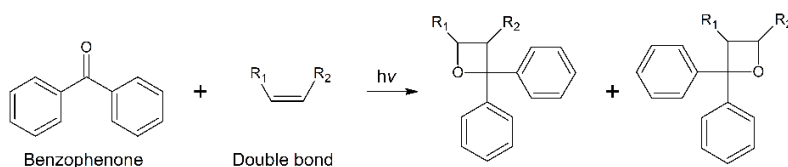


Analyte	OTCD Protocol			Matrix	Sample	Ref.
	Solution of derivatization reagent	Application method	Incubation or other treatment			
Arachidonic acid, cholic acid, citric acid, fumaric acid, glycocholic acid, glycerophosphocholine, lysophosphatidylcholine and others	TMPA 3 mM, HATU and HBOt at 1.5 mM in 90% ACN	Automatic Spraying	4 h at room temperature in a closed container with ACN gas	1,5 DAN 2 mg/mL in 80% ACN	Kidney and brain tissues from rats	Sun <i>et al.</i> ⁵⁹

Table 7. OTCD targeting double bond function

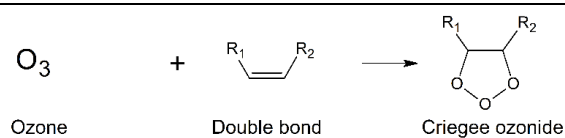
Double bond group					
a. Reaction with benzaldehyde					
<p style="text-align: center;">Benzaldehyde + Double bond $\xrightarrow{h\nu}$ Product 1 + Product 2</p>					
Analyte	OTCD Protocol		Matrix	Sample	Ref.
	Solution of derivatization reagent	Application method			
Phosphatidylcholine and phosphatidylserine isomers	Vapor of benzaldehyde	The reaction is carried out in a chamber equipped with a UV lamp with a peak emission at 254 nm	DHB application by sublimation	Brain tissues from C57BL/6 mice	Bednařik <i>et al.</i> ⁶⁰

b. Reaction with benzophenone (continued)



Analyte	OTCD Protocol			Matrix	Sample	Ref.
	Solution of derivatization reagent	Application method	Incubation or other treatment			
Phosphatidylcholine isomers	20 mg/mL in ACN/2-propanol/H ₂ O 6/3/1 + 0.5% TFA	Automatic Spraying	Irradiation by UV light for 3 min (254 nm)	Benzophenone as reactive matrix	Brain tissues from C57BL6/N mice and male <i>S. mansoni</i> tegument	Waldchen <i>et al.</i> ⁶²

c. Reaction with ozone (*continued*)



Analyte	OTCD Protocol	Matrix	Sample	Ref.
Phosphatidylcholine isomers	Ozone gas introduced in linear ion-trap	Mixture of sodium acetate (4 mg/mL) and norharmane matrix (7 mg/mL) in MeOH/CHCl ₃ (2/1)	Brains tissues containing tumors from ND2:SmoA1 transgenic mice	Paine <i>et al.</i> ⁶³
Phosphatidylcholine isomers (PCC 34:1)	Glass flask flushed with the flow of ozone from an ozone generator. Samples were allowed to react with ozone up to 30 min.	DHB deposition by sublimation	Brain tissues from BALB/c mice and colon tissue from patient	Bednařík <i>et al.</i> ⁶⁴

Table 8. OTCD targeting phosphate monoester function

Phosphahate monoester group						
Reaction with Phos-tag						
<p style="text-align: center;"> Phos-tag Phosphate monoester Phos-tag complex </p>						
Analyte	OTCD Protocol			Matrix	Sample	Ref.
	Solution of derivatization reagent	Application method	Incubation or other treatment			
Ceramide-1-phosphate, lysophosphatidic acid, phosphatidic acid sphingosine-1-phosphate	0.86 mg/mL in H ₂ O	Automatic Spraying	-	<i>para</i> -Nitroaniline 10 mg/mL in 80% EtOH + 150 mM ammonium formate	Brain tissues from ICR mice	Iwama <i>et al.</i> ⁶⁵

Table 9. OTCD targeting Diene function

Diene group of 25-hydroxyvitamin D						
Reaction with Ampiflex						
<p>The reaction shows Ampiflex (a dimethylamino-phenyl-alkoxy ketone) reacting with 25-hydroxyvitamin D (a complex steroid with a diene system). The product is a conjugated derivative where the diene system of the vitamin D is covalently bonded to the imine group of Ampiflex.</p>						
Analyte	OTCD Protocol			Matrix	Sample	Ref.
	Solution of derivatization reagent	Application method	Incubation or other treatment			
Vitamin D metabolites	Ampiflex 0.1 mg/mL in 50% ACN	Automatic Spraying	1 h at 37°C in a reaction container with ACN/H ₂ O solution	CHCA 5 mg/mL in 70% ACN + 0.1% TFA	Mouse kidney tissues	Smith <i>et al.</i> ⁶⁸

Table 10. OTCD targeting platinum-based compounds

Platinum-based compounds						
Reaction with DDTC						
<p>Oxaliplatin + DDTC $\xrightarrow[NaOH]{40\text{ }^\circ\text{C}}$ Pt(DDTC)₂ + Pt(DDTC)₃</p>						
Analyte	OTCD Protocol			Matrix	Sample	Ref.
	Solution of derivatization reagent	Application method	Incubation or other treatment			
oxaliplatin and its metabolites, cisplatin, and carboplatin	1% DDTC in 0.1 M NaOH	Airbrush deposition	5 min at 40°C in a humid environment	CHCA 10 mg/mL in 50% ACN + 0.1% TFA	3D multicellular tumor spheroid <i>in vitro</i> models	Liu <i>et al.</i> ⁷⁰

Table 11. OTCD targeting 3-methoxysalicylamine

Molecule targeted 3-methoxysalicylamine						
Reaction with TCDI						
<p style="text-align: center;"> <chem>C1=CN=C(S1)N2C=CN=C2</chem> + <chem>COc1cc(O)ccc1CN</chem> $\xrightarrow{\text{pH } 8.0}$ <chem>COc1cc(O)ccc1CN2C=CN=C(S2)</chem> </p> <p style="text-align: center;">TCDI 3-methoxysalicylamine 3-methoxysalicylamine-TCDI</p>						
Analyte	OTCD Protocol			Matrix	Sample	Ref.
	Solution of derivatization reagent	Application method	Incubation or other treatment			
3-methoxysalicylamine	10 mg/mL in 1:1 ACN/AMBIC	Automatic Spraying	30 min at 37°C in a humid environment	CHCA deposited by sublimation	Mouse kidney tissues	Chacon <i>et al.</i> ⁷¹

Table 12. OTCD targeting sialic acid in glycans

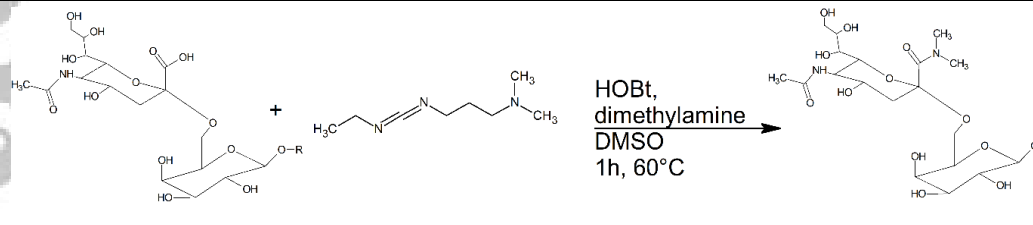
Sialic acid group in N-glycans				
Reaction with EDC				
 <p style="text-align: center;"> α2,6-linked sialic acid EDC </p>				
Analyte	OTCD Protocol	Matrix	Sample	Ref.
Sialylated N-glycans	<p>Incubation of tissue slides in 250 mM EDC, 500 mM HOBt and 250 mM dimethylamine in DMSO for 1 hour in 60°C oven</p> <p>Addition of 25% ammonia solution then 2 h incubation at 60°C</p>	<p>CHCA 5mg/mL in 50% ACN + 0.1% TFA</p>	<p>formalin-fixed and paraffin-embedded human colon carcinoma and leiomyosarcoma tissues</p>	<p>Holst <i>et al.</i>⁷²</p>

Table 13. Study of OTCD targeting the reducing terminus of N-glycan

The reducing terminus of N-glycan						
Reaction with GirP						
<p style="text-align: center;"> N-glycan GirP + H₂O </p>						
Analyte	OTCD Protocol			Matrix	Sample	Ref.
	Solution of derivatization reagent	Application method	Incubation or other treatment			
N-glycans (glucose, maltotriose, etc)	GirP 10 mg/mL in 50% MeOH + 10% acetic acid	Automatic spraying	30 min in chamber with acetic acid vapor	DHB 40 mg/mL in 70% MeOH + 0.1% TFA	formalin-fixed and paraffin-embedded (FFPE) human laryngeal cancer and ovarian cancer tissues	Zhang <i>et al.</i> ⁷⁴